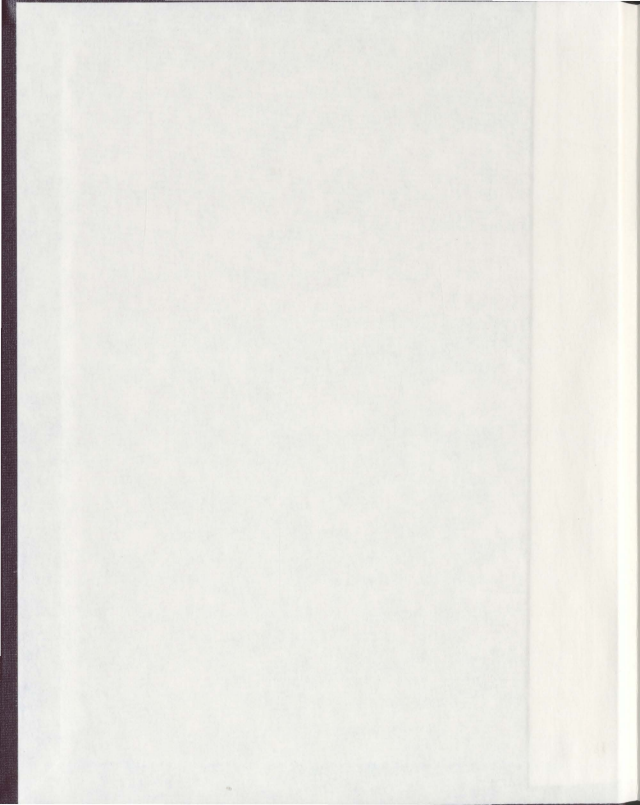


LACTATIONAL CHANGES IN THE BONE METABOLISM
OF MICE LACKING ONE COPY OF THE CALCITONIN
RECEPTOR GENE

YUE MA



LACTATIONAL CHANGES IN THE BONE METABOLISM OF MICE LACKING
ONE COPY OF THE CALCITONIN RECEPTOR GENE

by

© YUE MA

A thesis submitted to the

School of Graduate Studies

in partial fulfillment of the requirements for the degree of

Master of Science

Faculty of Medicine

Memorial University of Newfoundland

May 2012

St. John's

Newfoundland

ABSTRACT

Calcitonin plays a critical role in preventing excessive bone resorption during lactation. Mice lacking both copies of the calcitonin (CT) gene (CT null mice) lose 55% of bone mineral content (BMC) or twice the amount of wildtype mice during lactation. The calcitonin receptor (CTR) is expressed in the pituitary, lactating breast tissues and bone in mice. However, at which of the three tissues and through which mechanisms the calcitonin acts on CTR to regulate calcium metabolism during reproductive periods are still unclear. This project assesses mice lacking one copy of a CTR gene as a means to understand whether loss of CTR has the same phenotype as the loss of CT during the reproductive cycle. If so, it would enable more studies into the detailed mechanisms of how calcitonin works in each tissue during the reproductive period.

Wildtype (WT) and heterozygous *Ctr* gene-deleted sisters (*Ctr*^{+/-}) were used to compare BMC changes during pregnancy and lactation using the PixiMus DXA bone densitometer. *Ctr* null mice cannot be studied because they usually die prior to birth. Urine, serum and milk were collected and analyzed for the mineral content, bone formation, bone resorption markers, and parathyroid hormone (PTH). DXA scanning and urine/serum collections occurred at baseline (before pregnancy), late pregnancy, late lactation, and days 7, 14 and 21 of post-weaning recovery. Tibias were analyzed separately by micro-computed tomography (μ CT), the 3-point bend test, and real-time quantitative RT-PCR for *Ctr* gene expression.

WT and *Ctr^{+/-}* mice experienced typical lactational changes of BMC and bone microstructure and recovered quickly and fully to baseline levels after weaning. WT and *Ctr^{+/-}* females lost $10.7\% \pm 3.4\%$ and $10.6\% \pm 2.0\%$ BMC during lactation relative to baseline level respectively. No significant difference in BMC was observed between WT and *Ctr^{+/-}* mice at any time point. Urine calcium, phosphorus and magnesium levels changed appropriately during reproduction with no significant differences between WT and *Ctr^{+/-}*, except for significantly lower urine phosphorus (11.0 ± 2.2 of WT vs. 4.4 ± 1.4 of *Ctr^{+/-}*, $p < 0.05$) and a trend for lower urine calcium and magnesium in *Ctr^{+/-}* at late pregnancy. Bone turnover was increased in both genotypes at late lactation and early recovery. PTH showed an increasing trend from baseline to late lactation. Milk calcium content was the same in both genotypes. Bone strength was significantly decreased at late lactation with no difference between genotypes. WT and *Ctr^{+/-}* had equal levels of *Ctr* mRNA expression in the tibia.

In summary, WT and *Ctr^{+/-}* underwent similar changes in bone mass, bone microarchitecture, calciotropic hormones, and serum and urine minerals during pregnancy and lactation. After lactation, the skeleton of each genotype recovered fully and quickly. Loss of one copy of the calcitonin receptor gene does not cause the same phenotype as complete loss of the calcitonin gene (*Ctcgrp*), likely because one allele transcription of *Ctr* gene compensates.

ACKNOWLEDGEMENTS

I would like to thank my supervisor Dr. Christopher Kovacs: for providing me the research opportunity and taking me as a masters student and for trusting my research ability; for his excellent instruction, support, and supervision, under which I was able to attend the European Calcified Tissue Society Congress 2012; and, finally, I thank Dr. Kovacs for understanding and supporting my future plans. He provided me a valuable reference for my application to another academic program.

I would also like to thank my supervisory committee, Dr. Ann Dorward and Dr. Gary Paterno. Their comments and suggestions have helped me fulfill my master study.

I thank Dr. Deborah Galson at University of Pittsburgh. She kindly provided the mice for our use.

Also, I would like to thank Beth Kirby, the research assistant in our lab, for her guidance and assistance with many experimental techniques. Without her patience and help, I could not have carried out my experiments successfully.

At last, I thank my father and mother. Without your support and love, my study abroad would not have gone smoothly.

TABLE OF CONTENTS

ABSTRACT.....	ii
ACKNOWLEDGEMENTS.....	iv
TABLE OF CONTENTS.....	v
LIST OF FIGURES.....	x
LIST OF TABLES.....	xii
LIST OF ABBREVIATIONS.....	xiii
1 Introduction.....	1
1.1 Bone and mineral homeostasis.....	1
1.1.1 Bone.....	1
1.1.1.1 Bone structure and composition.....	1
1.1.1.2 Bone remodeling.....	2
1.1.1.2.1 Osteoblast.....	4
1.1.1.2.2 Osteoclast.....	4
1.1.1.2.3 Osteocyte.....	6
1.1.2 Calcium homeostasis.....	7
1.1.2.1 CaSR.....	7
1.1.2.2 Calcitriol.....	8
1.1.2.3 Parathyroid gland.....	9
1.1.2.4 Kidney.....	11
1.1.2.5 Intestine.....	12
1.1.2.6 Calcitonin.....	14
1.1.2.7 Calcitonin receptor.....	15

1.1.3 Phosphorus homeostasis	16
1.1.4 Magnesium homeostasis	18
1.2 Body adaption during reproductive period	19
1.2.1 During pregnancy	19
1.2.2 During lactation	21
1.2.3 During recovery after lactation	23
1.3 Animal model: CTR gene (<i>Ctr</i>) heterozygous mice.....	24
1.4 Project description	25
2 Materials and methods.....	27
2.1 Animal husbandry	27
2.2 Experimental time points.....	28
2.3 Genotyping	30
2.3.1 Tagging and tailing	30
2.3.2 DNA extraction	30
2.3.3 PCR.....	31
2.3.4 Gel electrophoresis.....	32
2.4 BMC measurement.....	33
2.5 Urine and serum collection.....	34
2.6 Milk collection.....	35
2.7 Bone tissue collection.....	35
2.8 Serum and urine total calcium measurement.....	36
2.9 Serum and urine inorganic phosphorus measurement.....	36
2.10 Serum and urine magnesium measurement.....	37

2.11 Urine creatinine measurement.....	37
2.12 Serum procollagen type 1 N-terminal propeptide (PINP) assay.....	38
2.13 Urine deoxypyridinoline (DPD) assay	39
2.14 Serum PTH assay	39
2.15 Milk protein measurement.....	40
2.16 Milk calcium measurement	40
2.17 Micro-computed tomography (μ CT).....	41
2.18 Biomechanical tests.....	42
2.18.1 3-point bend test.....	42
2.18.2 Reference point indentation test.....	42
2.19 <i>Ctr</i> gene expression analysis	43
2.19.1 RNA extraction	43
2.19.2 cDNA synthesis	43
2.19.3 Real-time quantitative RT-PCR.....	44
2.20 Statistical analysis	44
3 Results.....	46
3.1 Genotyping	46
3.2 Litter size	46
3.3 BMC measurement.....	49
3.4 Absolute BMC values.....	50
3.5 Serum and urine minerals assays.....	56
3.5.1 Serum total calcium	56
3.5.2 Urine calcium.....	56

3.5.3 Serum phosphorus.....	60
3.5.4 Urine phosphorus	60
3.5.5 Serum magnesium.....	60
3.5.6 Urine magnesium measurement.....	61
3.6 Markers of bone turnover assays.....	66
3.6.1 Serum PINP assay	66
3.6.2 Urine DPD	68
3.6.3 Serum PTH.....	68
3.7 Milk calcium content.....	68
3.8 Micro computed tomographic (μ CT) analysis of tibias.....	72
3.9 Biomechanical tests	74
3.9.1 3-point bend (3PB) test	74
3.9.2 Reference point indentation test.....	74
3.10 <i>Ctr</i> mRNA expression analysis	78
4 Discussion.....	80
4.1 Phenotypes in mice during reproductive period.....	80
4.2 Roles of <i>Ctr</i> in renal phosphorus excretion at late pregnancy	86
4.3 Parathyroid hormone during reproductive period	87
4.4 Comparison between <i>Ctr</i> ^{-/-} and Calcitonin (<i>Ct/cgrp</i>) knockout mice throughout reproductive period.....	89
4.5 Future work	91
4.5.1 Exploration of <i>Ctr</i> knockout mice on Blackswiss strain	91
4.5.2 Knockdown experiments?.....	92

4.5.3 Alternative global <i>Ctr</i> knockout which already exists.....	93
4.6 Conclusion.....	94
References.....	95

LIST OF FIGURES

Figure 1: Model of Bone Remodeling Compartment (BRC).....	3
Figure 2: Experimental design.....	29
Figure 3: Example of genotyping results.....	47
Figure 4: Litter sizes in WT and <i>Ctr^{+/-}</i> mice at Late Lactation.....	48
Figure 5: BMC (g) in WT and <i>Ctr^{+/-}</i> mice at Baseline	51
Figure 6: Whole body BMC changes relative to BMC at Baseline throughout reproductive period	52
Figure 7: Lumbar spine BMC changes relative to BMC at Baseline throughout reproductive period	53
Figure 8: Hind limb BMC changes relative to BMC at Baseline during reproductive period	54
Figure 9: Absolute whole body BMC values (g) in WT and <i>Ctr^{+/-}</i> mice throughout the reproductive period	55
Figure 10: Serum total calcium in WT and <i>Ctr^{+/-}</i> mice throughout reproductive period ..	58
Figure 11: Urine calcium in WT and <i>Ctr^{+/-}</i> mice during reproductive period	59
Figure 12: Serum phosphorus in WT and <i>Ctr^{+/-}</i> mice throughout the reproductive period	62
Figure 13: Urine phosphorus in WT and <i>Ctr^{+/-}</i> mice throughout the reproductive period.	63
Figure 14: Serum magnesium in WT and <i>Ctr^{+/-}</i> mice throughout reproductive period.....	64
Figure 15: Urine magnesium in WT and <i>Ctr^{+/-}</i> throughout the reproductive period	65
Figure 16: Serum P1NP in WT and <i>Ctr^{+/-}</i> mice throughout the reproductive period.....	67
Figure 17: Urine DPD in WT and <i>Ctr^{+/-}</i> mice during the reproductive period.....	69
Figure 18: Serum PTH in WT and <i>Ctr^{+/-}</i> mice throughout the reproductive period.....	70
Figure 19: Milk calcium content normalized to milk protein in WT and <i>Ctr^{+/-}</i> mice at Early Lactation.....	71

Figure 20: Indentation distance increase of tibiae at Baseline and Late Lactation in WT mice.....	77
Figure 21: Tibial expression of CTR mRNA in WT and <i>Ctrl</i> ^{-/-} at Baseline	79

LIST OF TABLES

Table 1: Micro computed tomographic changes in WT and <i>Ctrl</i> ^{+/+} mice at Baseline and Late Lactation (LL).....	73
Table 2: 3-point bend (3PB) test of tibia between WT and <i>Ctrl</i> ^{+/+} at Baseline and Late Lactation (LL).....	76

LIST OF ABBREVIATIONS

25-hydroxyvitamin D-1 α hydroxylase.....	1 α (OH)ase
3-point bend test.....	3PB test
3' Untranslated region.....	3' UTR
Alkaline phosphatase.....	ALP
Analysis of variance.....	ANOVA
Bone mineral content.....	BMC
Bone mineral density.....	BMD
Bone remodeling compartment.....	BRC
Bone surface.....	BS
Bone volume.....	BV
Bone volume/tissue volume.....	BV/TV
C57BL/6J inbred strain.....	C57
Ca ²⁺ -sensing receptor.....	CaSR
Calcitonin.....	CT
Calcitonin gene related peptide α	CGRP α
Calcitonin gene.....	<i>Ct/cgrp</i>
Calcitonin receptor.....	CTR
Calcium-binding proteins.....	Calbindins
Centimeter.....	cm
Chloride ion.....	Cl ⁻
Cortical thick ascending limb.....	CTAL

CTR gene.....	<i>Ctr</i>
Cytomegalovirus.....	CMV
Day(s).....	d
Deoxyadenosine triphosphate.....	dATP
Deoxycytidine triphosphate.....	dCTP
Deoxyguanosine triphosphate.....	dGTP
Deoxyribonucleic acid.....	DNA
Deoxyribonucleotide triphosphates.....	dNTPs
Deoxythymidine triphosphate.....	dTTP
Deoxypyridinoline.....	DPD
Distal convoluted tubule.....	DCT
Dual energy X-ray.....	DXA
Ethanol sodium acetate.....	EtOH:NaOAc
Enzyme immunoassay.....	EIA
Enzyme-linked immunosorbent assay.....	ELISA
Ethylenediaminetetraacetic.....	EDTA
Extracellular fluid.....	ECF
Extracellular matrix.....	ECM
Extracellular signal-regulated kinase 1/2.....	ERK 1/2
Fibroblast growth factor 23.....	FGF23
Fluorescent reporter dye 6-carboxylfluoresceine.....	FAM
Glyceraldehyde-3-phosphate dehydrogenase.....	GAPDH
Gram(s).....	g

Hematopoietic stem cells.....	HSCs
Heterozygous.....	HET
Horseradish peroxidase.....	HRP
Hour(s).....	h
Interleukin.....	IL
Ionized calcium.....	Ca ²⁺
Jun N-terminal kinase.....	JNK
Late Lactation.....	LL
Macrophage-colony stimulating factor.....	M-CSF or CSF-1
Magnesium.....	Mg
Mean trabecular separation.....	MTS
Mean trabecular thickness.....	MTT
Micro-computed tomography.....	μCT
Microgram(s).....	μg
Microliter.....	μL
Milliliter.....	ml
Millimolar.....	mM
Minor groove binder.....	MGB
Minute(s).....	min
Mitogen-activated protein kinase.....	MAPK
Nanometer.....	nm
Na-phosphate cotransport system.....	NPT – 2
Neomycin cassette.....	Neo

NF- κ B ligand.....	RANKL
Nuclear factor - κ B.....	NF- κ B
Osteonectin.....	ON
Osteopontin.....	OPN
Osteoprotegerin.....	OPG
Parathyroid hormone.....	PTH
Phosphate.....	Pi
Plasma membrane calcium ATPase.....	PMCA1b
Potassium chloride.....	KCl
Polymerase chain reaction.....	PCR
Procollagen type 1 N-terminal propeptide.....	P1NP
PTH-related peptide.....	PTHrP
PTH/PTHrP receptor.....	PTHrR
Pyridinoline.....	PYD
Real-time PCR.....	RT-PCR
Receptor modulating proteins.....	RMPs
Receptor-activity-modifying proteins.....	RAMPs
Reference point indentation test.....	RPI test
Revolution per minute.....	rpm
Retinoid X receptor.....	RXR
Ribonucleic acid.....	RNA
Second(s).....	s
Sodium-calcium exchanger.....	NCX1

Sodium dodecyl sulfate.....	SDS
Standard error.....	SE
Tissue volume.....	TV
Transforming growth factor – β	TGF – β
Transient receptor potential cation channel, superfamily M, member 6 protein.....	TRPM6
Transient receptor potential vanilloid type 5.....	TRPV5
Transient receptor potential vanilloid type 6.....	TRPV6
Tris-acetate-EDTA.....	TAE
Type 1 collagen.....	Col1
Uracil-N-glycosylase.....	UNG
Vitamin D receptor.....	VDR
Week(s).....	wk
Wildtype.....	WT

1 Introduction

1.1 Bone and mineral homeostasis

1.1.1 Bone

Bone plays physiologically essential roles in vertebrate animals. It protects internal organs, provides frames to which internal organs can attach, and is a reservoir of minerals such as calcium, phosphorus and magnesium.

1.1.1.1 Bone structure and composition

Morphologically, bone can be divided into two forms: cortical and cancellous (also called trabecular). Cortical bone exists on the outer shell of most bones and accounts for 80% of the weight of the human skeleton; cancellous bone is located in the interior of bone and contributes to the rest of the human skeleton's weight (1). Cancellous bone has a looser and more porous structure than cortical bone. The ratio of surface to volume in cancellous bone is much greater than that in cortical bone, thus enabling cancellous bone to be readily resorbed by osteoclasts and to be more physiologically active, such as releasing alkali or minerals when needed. The different morphology of the two forms of bone leads to different primary functions: Cortical bone provides support and protection of internal organs while cancellous bone provides metabolic functions (2). Both forms contribute to the overall strength of bone.

Bone contains 4 types of cells: osteoblasts, osteoclasts, bone lining cells and osteocytes. Osteoblasts differentiate from mesenchymal precursor cells (3), which exist at the bone surface. Unlike osteoblasts, osteoclasts belong to the monocyte/macrophage family and are derived from hematopoietic stem cells (HSCs) (4). Bone lining cells are flat and inactive, covering the non-remodeling surface of bone. They may become reactivated as osteoblasts. Osteocytes are derived from osteoblasts, which form bone and account for 90 – 95% of all bone cells in a human adult skeleton (5). Unlike osteoblasts, osteoclasts, and bone lining cells, osteocytes exist in the interior of bone.

1.1.1.2 Bone remodeling

Bone is continuously remodeled during life with simultaneous bone formation and resorption. Bone remodeling provides many benefits *in vivo*: it releases calcium from bone into serum to maintain calcium homeostasis, repairs microfractures that occur from daily physical activities, and replaces old bone. Bone remodeling has its own unique structure called the Bone Remodeling Compartment (BRC) (6). The BRC is covered by lining cells, which have similar characteristics to bone lining cells, and mainly consists of osteoclasts at the forward (cutting/drilling) end, with osteoblasts following after (see Figure 1). This structure enables bone remodeling to work efficiently to maintain normal bone physiological activities.

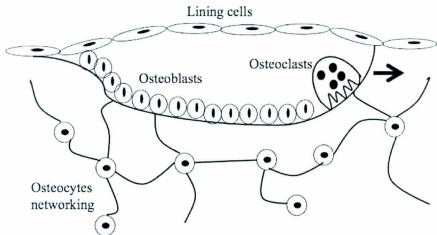


Figure 1: Model of Bone Remodeling Compartment (BRC). BRC mainly consists of lining cells, osteoblasts, and osteoclasts. Osteoblasts follow osteoclasts. The black arrow indicates the direction of movement of the osteoclasts.

1.1.1.2.1 Osteoblast

Osteoblasts form new bone. As new bone is formed, mesenchymal stem cells differentiate toward mature osteoblasts. These osteoblasts proliferate and lay down extracellular matrices (ECM), which then becomes mineralized (7). Any factors affecting osteoblast differentiation will affect bone formation. Runx2 (Cbfa1) is a transcription factor that triggers downstream cell signal cascades to express osteoblast specific genes, such as type I Collagen (Col1), alkaline phosphatase (ALP), osteopontin (OPN), osteonectin (ON) and osteocalcin (3). The critical importance of Runx2 for osteoblasts and bone formation was shown by *Runx2^{-/-}* mice, which died of respiratory failure due to lack of osteoblasts, bone, and, therefore, a solid rib cage (8). However, Runx2 is not the only regulator. Osterix is downstream of Runx2 in the mesenchymal stem cell differentiation pathway (9). Absence of Osterix can also lead to deficiencies during bone formation (10). Runx2 and the Runx2/Osterix pathway function together to support bone formation through regulation of osteoblast differentiation. Besides these two major regulators, Runx2 and Osterix, there are still other factors that participate in the regulation of osteoblast differentiation. For example, bone morphogenic proteins, which belong to TGF- β superfamily, have a positive effect on osteoblast differentiation by increasing bone formation (11, 12).

1.1.1.2.2 Osteoclast

A primary function of osteoclasts is to resorb bone through the production of powerful enzymes and acids. Bone resorption by osteoclasts requires tight physical contact between osteoclasts and bone matrices using integrin $\alpha\beta3$ to create a sealed zone under the

osteoclast (13), and the formation of a microenvironment with a pH as low as 4.5, established by proton pumps and Chloride (Cl⁻) Channels (4). The acidified environment releases the mineral content in bone and exposes the organic matrix that is mainly made of type 1 collagen. Type 1 collagen is further degraded by the lysosomal enzyme cathepsin K.

Osteoclast differentiation is related to bone resorption activities. The two major cytokines that regulate differentiation are Macrophage-Colony Stimulating Factor (M-CSF or CSF-1) and Receptor Activator of NF- κ B Ligand (RANKL). M-CSF itself induces the formation of osteoclast progenitors from hematopoietic stem cells (HSCs) (14, 15). RANKL is an essential factor for the differentiation of osteoclasts, from small cells to large multinucleated mature osteoclasts. By binding to its receptor (RANK), RANKL increases the expression of several osteoclast-specific genes to induce osteoclast differentiation (15). Osteoprotegerin (OPG) inhibits the RANK/RANKL pathway by acting as a high affinity decoy receptor to RANKL. The ratio of RANKL to OPG is a key factor in osteoclast formation and the regulation of bone resorption (4). In addition to the two key cytokines M-CSF and RANKL, other molecules such as interleukin (IL)-1, parathyroid hormone (PTH), PTH-related peptide (PTHrP), and calcitriol also regulate the differentiation of osteoclasts (16-18). The calcitonin receptor is expressed at the surface of osteoclasts, indicating that calcitonin has certain roles in osteoclasts (19). One study showed that calcitonin could inhibit both osteoclast formation and multinucleated osteoclast formation by activating the cAMP-PKA pathway, which stimulated the phosphorylation of Extracellular signal-regulated kinase 1/2 (ERK 1/2) (activated form),

and inducing Epac, which activated ERK1/2 (20). However, the full mechanism of how calcitonin inhibits osteoclasts is still unclear. The function of calcitonin will be further discussed in the Calcitonin Section (1.1.2.6).

1.1.1.2.3 Osteocyte

Osteocytes form from osteoblasts which become embedded in the bone matrix and communicate with each other through thousands of canaliculi, much like neurons communicate with each other (21). Generally speaking, osteocytes are the master controllers of bone remodeling. Osteocytes regulate bone remodeling by sensing the loading force and then send bone formation signals to recruit osteoblasts (22). Osteocyte-ablated mice are resistant to unloading (tail suspension)-induced bone resorption, which suggests that it is the osteocyte that senses loading force (23). Osteoclast activity is inhibited by osteocyte-like cell conditioned medium, and the inhibitory effect enhanced by estrogen is due to TGF- β 3 being secreted by the osteocyte-like cells (24). Ablation of osteocytes increases osteoclast activity dramatically *in vivo*, resulting in high levels of bone resorption (23). Osteocyte death and apoptosis also stimulate bone resorption. Micro-damage and micro-cracks are thought to break canaliculi, thus physically damaging osteocytes and then causing osteocyte apoptosis. This was shown in the observation of apoptotic osteocytes at micro-damage sites *in vivo* (25). Simultaneous osteocyte apoptosis and unloading send signals to recruit and activate osteoclasts to increase bone resorption (5, 26).

1.1.2 Calcium homeostasis

Bone is the main calcium storage site of the body. Ninety-nine percent of calcium is stored in bone as hydroxyapatite crystals in the human body. The remaining 1% of calcium exists in blood, extracellular fluid, and soft tissue (27). Of the calcium in blood, 45% is bound to albumin, 10% is bound to small molecules such as phosphate and citrate, and the remaining 45% is free or ionized in a biologically active form (27). Ionized calcium is maintained at a stable level *in vivo* due to the action of the Ca^{2+} -sensing receptor (CaSR).

1.1.2.1 CaSR

The CaSR is expressed by the parathyroids, kidneys, intestine, thyroid gland, and bone (28). The primary function of this receptor is to sense the ionized calcium (Ca^{2+}) concentration and maintain it at a constant level *in vivo*. The CaSR appears to regulate the cells and tissues that are needed to increase or decrease serum calcium. For example, it inhibits parathyroid hormone (PTH), increases urine calcium excretion, stimulates calcitonin, and probably alters osteoclast and osteoblast activity (29). The biologically active form of the CaSR is a dimer at the cell surface. The dimer is not formed until Ca^{2+} concentration in extracellular fluid (ECF) is high (30). Activation of the CaSR induces several G-protein mediated pathways, including mitogen-activated protein kinase (MAPK) cascades. ERK 1/2 and Jun N-terminal kinase (JNK) are translocated into the nucleus to modify targeted gene expression (31). A high Ca^{2+} concentration in ECF can reduce PTH gene expression and stimulate calcitonin release.

1.1.2.2 Calcitriol

Calcitriol, also known as 1,25-dihydroxyvitamin D₃, plays an essential role in maintaining calcium homeostasis *in vivo*. It is the biologically active form of Vitamin D₃. The key enzyme involved in this conversion process is 25-hydroxyvitamin D-1 α hydroxylase [1 α (OH)ase] which converts 25-hydroxy-Vitamin D₃ into calcitriol. Calcitriol belongs to the steroid hormone family and acts on Vitamin D receptors (VDR) located in the cytoplasm. Once calcitriol binds to VDR, the complex enters the nuclei of cells and forms a heterodimer with the retinoid X receptor (RXR) to activate Vitamin D target genes (32). The classical target tissues of calcitriol are bone, intestine, and kidney. Calcitriol's main effects on bone are thought to be indirect, stimulating the absorption of calcium and phosphorus from the intestine. Studies in humans and animals have shown that the skeletal effects of severe vitamin D deficiency or absence of the vitamin D receptor can be completely reversed by intravenous calcium infusions or a high calcium diet (33, 34). However, *in vitro* experiments have shown that calcitriol can stimulate bone formation and resorption. On one hand (bone formation), it increases the level of calcium-binding proteins, osteocalcin, and osteopontin in osteoblasts (35, 36). Elevated osteocalcin and osteopontin accelerate the process of mineralization to form new bone. On the other hand (bone resorption), RANKL expression at the surface of osteoblasts is enhanced by calcitriol. Physical cell-to-cell contact between osteoblasts with high RANKL and osteoclast precursors induces more osteoclast formation, thus increasing bone resorption (37). Runx2 expression is also suppressed by calcitriol to reduce osteoblast differentiation (38). The net effect of calcitriol's direct actions on osteoblasts and osteoclasts may be small or even neutral *in vivo*. However, these actions may explain why extremely high

levels of calcitriol can cause significantly increased bone resorption in patients with sarcoidosis or hypervitaminosis D (39, 40).

In the kidneys, calcitriol enhances PTH's effect on calcium reabsorption in distal tubules by increasing PTH receptor expression (41). The function of PTH on calcium reabsorption in the kidneys will be discussed in the Kidney Section 1.1.2.4. Calcitriol also increases renal expression of calcium-binding proteins (calbindins) (42). The increased calbindins transfer more calcium from the lumen in distal tubule to blood; therefore, more calcium is reabsorbed. However, calcitriol inhibits $1\alpha(\text{OH})\text{ase}$ activity and stimulates the catabolic enzyme 24-hydroxylase (43). These mechanisms make sure that the calcitriol level *in vivo* is maintained within a normal range.

The effect of calcitriol on the intestine will be discussed in the Intestine Section 1.1.2.5.

1.1.2.3 Parathyroid gland

Parathyroid glands play an important role in calcium homeostasis *in vivo*—they secrete PTH. PTH is a key factor in regulating calcium homeostasis *in vivo* as it regulates bone formation and resorption, increases reabsorption of calcium and excretion of phosphorus by kidney tubules, and indirectly stimulates intestinal calcium absorption by increasing renal expression of 1α hydroxylase to form calcitriol (44). The function of PTH is coupled with the expression of the CaSR at the surface of chief cells in parathyroid glands. Activation of the CaSR by a high serum calcium level inhibits PTH synthesis, secretion,

and parathyroid cell growth. When a low serum calcium concentration is present, CaSR is not activated, and so more PTH will be produced and released to raise blood calcium.

In bone, the PTH/PTHrP receptor (PTHrP) is expressed by osteoblasts. However, the actions of PTH are complex. In response to PTH, osteoblast apoptosis is inhibited. As well, osteoblasts proliferate, and their activity is increased to lay down matrix and form bone; in the absence of PTH, osteoblasts are inactive and little new bone is formed (45). Also in response to PTH, osteoblasts are stimulated to produce RANKL, which binds to RANK on the surface of osteoclast precursors and mature osteoclasts. As discussed above, the net effect of this means increased numbers of mature osteoclast cells that are recruited to the bone surface to resorb bone. PTH also reduces osteoblasts' expression of OPG (46, 47), thus making the ratio of RANKL to OPG high. Which of these opposing actions of PTH predominates (to stimulate bone formation or, conversely, to stimulate bone resorption) may depend upon the circulating level of PTH or some aspect of the magnitude and frequency of its pulsed release. This has been confirmed by experiments in animals that demonstrated that one- or two-hour infusions of PTH increased osteoblast activity without affecting osteoclast activity, while longer infusions of PTH markedly increased osteoclast activity (48). Also, once-daily injections of PTH markedly stimulated bone formation and led to a massive increase in bone mass (47, 49). In humans, once-daily subcutaneous injections of PTH induce net bone formation and have become a standard treatment for osteoporosis, while chronically elevated PTH due to primary or secondary hyperparathyroidism leads to increased bone resorption and net bone loss (50-52). Therefore, it is evident that PTH's opposing actions on osteoblasts may depend upon

the magnitude and frequency of its release, but the detailed mechanisms of this relationship are still unclear.

The function of PTH in both the kidney and the intestine will be discussed in the following Kidney Section 1.1.2.4 and Intestine Section 1.1.2.5.

1.1.2.4 Kidney

The kidneys regulate calcium balance by reabsorbing and excreting calcium. Sixty-five percent of filtered calcium is reabsorbed at proximal tubules, 20% at cortical thick ascending limbs (CTAL), and the remaining 15% at distal convoluted tubules (DCT) (27). PTH has no effect on calcium reabsorption at the proximal tubules. In CTAL, calcium reabsorption is driven by the Na-2Cl-K cotransporter. The cotransporter mainly regulates NaCl reabsorption, but the electrochemical gradient formed by NaCl reabsorption enables calcium to be reabsorbed. PTH increases calcium reabsorption at the CTAL by enhancing the activity of the Na-2Cl-K cotransporter (53, 54). Conversely, the CaSR inhibits the overall activity of the Na-2Cl-K cotransporter at the CTAL such that less calcium is reabsorbed. In the DCT, calcium reabsorption is an active and transcellular process enabled by several Ca-transporting proteins including transient receptor potential vanilloid type 5 (TRPV5), TRPV6, plasma membrane calcium ATPase (PMCA1b), sodium-calcium exchanger (NCX1) and calbindin-D28K (55). NCX1 is a ubiquitously expressed cell membrane protein that trades three sodium ions for one calcium ion. PTH primarily increases the activity of NCX1 at DCT (27), thus causing increased sodium

excretion to enable more calcium to be absorbed. It is unclear whether the CaSR has any actions of calcium reabsorption at the DCT (28).

The effect of PTH on renal calcium reabsorption might seem insignificant given that 65% of calcium is reabsorbed in the proximal tubules independently of PTH, and that the CaSR has actions which oppose PTH in CTAL (27, 56). However, the critical importance of PTH on renal calcium handling is made clear by what happens when PTH concentrations are low or absent, such as in hypoparathyroidism: the serum calcium becomes very low, which should prompt the kidneys to avidly conserve calcium, but instead urine calcium excretion increases markedly, thereby worsening the calcium deficit and hypocalcemia (57).

1.1.2.5 Intestine

The intestines absorb calcium from the diet. Ninety percent of this absorption occurs at the duodenum and jejunum in humans, and the duodenum in mice. This absorption includes passive, paracellular and active, transcellular mechanisms. The passive pathway is driven by electrochemical gradients caused by high Ca^{2+} concentration of $1\text{-}5\times 10^{-3}\text{M}$ in the intestinal lumen and low Ca^{2+} concentration of 10^{-3}M in blood. This pathway is utilized by administering a high calcium diet to bypass the effect of the absence of calcitriol. The active pathway involves membrane receptors and cytosol binding proteins. Ca^{2+} concentration differences between intestinal lumen ($1\text{-}5\times 10^{-3}\text{M}$) and cytosol (10^{-6}M) force calcium into intestinal epithelial cells through the calcium channel TRPV6, also

known as CAT1 or ECaC2, at the cell membrane (58-60). Once calcium is absorbed into epithelial cells, it is bound to Calbindin-D_{9k} and other calbindins, which carry calcium from the apical membrane to the basolateral membrane (60). Calcium is then pumped out of cells by the Ca²⁺-ATPase (PMCA1b) at basolateral membranes. The Na-Ca exchanger (NCX1) may also play a minor role in pumping out calcium from intestinal epithelial cells (54). However, despite decades of research, the mechanisms explaining the active, transcellular route remain uncertain. This is shown by the fact that loss of either TRPV6 or Calbindin-D_{9k} does not decrease intestinal calcium absorption, but loss of both TRPV6 and Calbindin-D_{9k} does decrease the calcium absorption (61).

Calcitriol is a critical stimulator of the active calcium absorption pathway in the intestine. Calcitriol goes into the brush border cells to bind VDR, thus initiating downstream transcription regulation (62). This process increases the expression of TRPV6, Calbindin-D_{9k}, PMCA1b, and other proteins, thus causing calcium to be more efficiently absorbed at the small intestine (63, 64). If VDRs are absent (so that calcitriol cannot act) or severe Vitamin D deficiency is present (so that calcitriol is reduced or absent), intestinal calcium absorption is significantly impaired, and hypocalcemia results. Calcitriol's role in stimulating the active pathway is critical because dietary calcium intake is normally well below the amount needed for the passive pathway to absorb the amount required.

As noted earlier, PTH indirectly regulates the active, transcellular transportation of calcium by increasing 1 α (OH)ase expression, leading to enhanced synthesis of calcitriol

(65). Direct actions of PTH to stimulate intestinal calcium absorption have been proposed, but have not been confirmed.

1.1.2.6 Calcitonin

Calcitonin was first purified by Copp and Cheney in 1962 (66, 67). Early experiments showed that injection of commercial thyroid extract into dogs caused transient hypocalcemia, and perfusion of blood containing high calcium into the thyroid and parathyroid glands of dogs resulted in a systemic fall in blood calcium. These results indicated that calcitonin was a hormone that lowered the blood calcium and was secreted by thyroid gland (66, 67). Calcitonin was also thought to have the opposite actions of PTH. Later studies showed that it is the C-cells of the thyroid gland that produce calcitonin and not the cells that produce the thyroid hormone (68, 69). More recently, it has been discovered that the brain, lactating breast, and placenta can also contribute to calcitonin production to some extent. Within the C-cells at least, the CaSR responds to an increase in serum calcium by stimulating the synthesis and release of calcitonin.

Calcitonin is a 32 amino acid peptide and expressed by the *ct/cgrp* gene located at human chromosome 11. An alternative splicing product of the *ct/cgrp* gene is calcitonin gene related peptide α (CGRP- α); it is produced by the nervous system and may not play a significant role in calcium or bone metabolism. Calcitonin's actions to oppose PTH occur in the kidney and osteoclasts. It can inhibit proximal tubular reabsorption of calcium to

increase urine calcium by effects on Na-H exchangers, and it directly inhibits osteoclasts to decrease bone resorption (56, 70, 71).

Following Copp's initial discoveries, it became evident that the ability of calcitonin to lower blood calcium was only seen with pharmacological dosages in humans. This led to the historical view that calcitonin is physiologically unimportant *in vivo* (72). This viewpoint was based on the fact that surgical removal of thyroid glands does not cause hypocalcemia or any obvious bone phenotype (73-75). However, these experiments overlooked more recently recognized calcitonin sources such as the breast and placenta. Increased calcitonin gene expression in lactating breast tissue elevates calcitonin in the serum of women who had a thyroidectomy (76). The surgical models of calcitonin deficiency were not truly devoid of calcitonin, especially during pregnancy and lactation. More recent studies using gene targeting techniques have shown that calcitonin may function in mammals during reproductive periods. Previous studies in our lab showed that calcitonin could protect bone from excessive resorption during lactation. Female *ct/cgrp* knockout mice do not make calcitonin. They lost twice as much BMC during lactation as their normal sisters did, and treatment with exogenous calcitonin rescued the massive bone resorption phenotype (77).

1.1.2.7 Calcitonin receptor

The calcitonin receptor (CTR) belongs to the 7-transmembrane and G-protein coupled receptor family (78). CTRs are expressed at renal proximal tubules, osteoclasts in bone

tissue, mammary tissue, placenta, and pituitary (78-81). Receptor modulating proteins (RMPs) heterodimerize with CTR to create isoforms of CTR (82, 83). Several proteins including CGRP-receptor component protein and receptor-activity-modifying proteins (RAMPs) belong to RMPs (82).

1.1.3 Phosphorus homeostasis

Calcium and phosphorus metabolisms are interlinked since both are needed to mineralize bone, and both are present in blood at concentrations that could cause damaging calcium-phosphorus crystals to form. Phosphorus is abundant *in vivo*. Most of phosphorus is stored in bone with calcium in the form of hydroxyapatite crystals. The remainder largely exists in soft tissue, and less than 1% of phosphorus is in the ECF. There are two forms of phosphorus in ECF: the organic form of phospholipids and the inorganic form of phosphate (Pi). Pi homeostasis is critical *in vivo*, and any disorder of Pi homeostasis will affect almost all organs. Maintenance of Pi homeostasis keeps phosphorus within a narrow range of 2.4 – 4.1 mg/dL (84).

Several factors can affect Pi homeostasis. Under extreme conditions of phosphorus deficiency, bone will break down to support the blood phosphorus level. In normal conditions, the two pathways that regulate Pi homeostasis are intestinal absorption and renal reabsorption. Intestinal absorption includes paracellular, passive absorption that depends on diffusional flux and transcellular, active absorption that is calcitriol-dependent and requires Na-P-binding protein (85, 86). Calcitriol stimulates the active

absorption of phosphorus, however, the detailed mechanism needs further research (87). On a normal diet, the phosphorus content usually exceeds daily needs such that passive absorption is usually sufficient. Calcitriol's role to stimulate active absorption is normally not essential.

The majority of renal excretion occurs at proximal tubules, and the rest of Pi is reabsorbed at proximal straight tubules and distal tubules. Reabsorption at all three sites is driven by specific phosphate channels called the Na-Phosphate cotransport system (NPT-2) (88). PTH decreases the reabsorption of Pi by inhibiting NPT-2 expression and activity at the 3 sites (89). This inhibition is thought to be related to the cAMP pathway induced by activation of the PTHR.

Fibroblast growth factor23 (FGF23) is a newly recognized and important factor regulating Pi reabsorption in kidneys. It lowers the serum phosphorus by reducing renal Pi reabsorption. This has been confirmed by human disorders and animals models, which revealed that excess FGF23 action cause hypophosphatemia and renal phosphorus wasting, whereas absence of FGF23 leads to impaired renal phosphorus excretion and hyperphosphatemia (90). FGF23 suppresses NPT-2 (91) and has negative effects on calcitriol by inhibiting $1\alpha(OH)ase$ activity (92). Reduced calcitriol contributes to renal phosphate wasting and also leads to reduced Pi absorption at the small intestine. Binding of FGF23 with its receptor in kidneys requires the existence of a co-factor called α -Klotho (93). α -Klotho is also found in parathyroid cells where FGF23 appears to suppress PTH.

Both PTH and FGF23 play critical roles in phosphorus homeostasis since loss of either leads to increased serum Pi level due to decreased urine Pi excretion.

1.1.4 Magnesium homeostasis

The human body is rich in magnesium (Mg). Sixty-six percent is located in bone, thirty-three percent is intracellular and the remaining one percent exists in ECF including serum. Of the Mg in serum, 30% is bound to protein and 70% is ionized. Magnesium can suppress PTH release by acting on the CaSR, but it does not do so as effectively as ionized calcium (27).

Mg homeostasis depends on the balance between intestinal absorption and renal handling. Like Ca and Pi, Mg is absorbed by two pathways in the small intestine: a paracellular, passive process driven by the Mg concentration in the intestinal lumen and an active transcellular process mediated by transient receptor potential cation channel, subfamily M, member 6 protein (TRPM6) (94). Calcitriol increases Mg absorption at the small intestine, but whether PTH is involved in the process is still unclear (27, 95). The majority of Mg reabsorption in the kidney occurs at the CTAL, with the remaining Mg reabsorbed at the proximal tubule and DCT. TRPM6 is expressed in the DCT, suggesting a role in Mg reabsorption at this site (94). PTH increases Mg reabsorption to some extent in the kidney, but is not a physiologically important factor (96). The reabsorption can be suppressed

partially by activation of the CaSR located at the proximal tubule, CTAL and DCT (97, 98).

1.2 Body adaptation during reproductive period

Reproduction involves unique adaptations to calcium and bone metabolism in female mammals. The reproductive period can be divided into three phases: pregnancy, lactation and recovery after lactation. During pregnancy, the mother provides minerals for fetal development mainly through increased efficiency of intestinal absorption; during lactation, the mother mobilizes calcium from bone to provide to milk; after lactation, the maternal skeleton recovers from bone loss incurred during pregnancy and lactation. For each stage, the strategies used by the maternal body are different.

1.2.1 During pregnancy

The pregnant mammal adopts several strategies to maintain calcium homeostasis during pregnancy. Intestinal absorption of calcium is dramatically increased (99). The rate of this intestinal absorption is elevated as early as 12 weeks into gestation in humans and remains at a high level throughout pregnancy (100). The dietary calcium intake of pregnant women is often higher than prior to pregnancy if nutrition guidelines are followed, and this may enhance the paracellular diffusion of calcium from intestinal lumen to blood due to a high calcium electrochemical gradient in the lumen. Calcitriol levels are 2 to 5 times higher during pregnancy, and this may explain increased expression of TRPV6 and Calbindin-D_{9k} at the intestinal epithelial cells. The increased

TRPV6 and Calbindin- D_{9k} induce more calcium absorbed by the transcellular, active way. PTH related peptide (PTHrP) may also participate in the increased intestinal absorption of calcium. It has structural similarity to PTH, enabling PTHrP to mimic PTH's actions on the kidney to raise $1\alpha(\text{OH})\text{ase}$ expression and activity (101-103). Elevated $1\alpha(\text{OH})\text{ase}$ catalyzes more calcitriol production, which in turn increases intestinal absorption. Other factors such as high estradiol, prolactin, and placental lactogen have been shown to stimulate $1\alpha(\text{OH})\text{ase}$ expression. It is also evident that high levels of calcitriol may not fully explain increased intestinal calcium absorption during pregnancy, since severely vitamin D deficient rats and *Vdr* null mice each upregulate intestinal calcium absorption to normal levels during pregnancy (104, 105). Prolactin, placental lactogen and other factors may stimulate intestinal calcium absorption through direct actions on enterocytes (intestinal absorptive cells). Generally speaking, both paracellular and transcellular calcium transportation contribute to the increased calcium absorption at the intestine.

The skeleton may also contribute calcium during pregnancy, but the extent to which this happens in women is uncertain. Most studies have measured bone mineral content (BMC) or bone mineral density (BMD) prior to pregnancy and 2 – 6 weeks after, with minimum change to as much as a 4% decrease observed. The concern about fetal radiation exposure limits such experimental data. Animal studies have shown that the skeletal response to pregnancy depends partially on genetic background. Outbred Blackswiss mice gained BMC by nearly 20% in the whole body and spine during pregnancy, suggesting that the mother stores bone minerals, mainly calcium, to prepare for massive bone calcium loss during lactation due to milk production (77). Conversely, our lab has also found that

inbred C57BL/6J mice gain BMC at the whole body level but lose 10-15% at the spine during pregnancy. The Wysolmerski lab has found that inbred CD1 mice have no change in BMD during pregnancy (106).

The increased intestinal absorption of calcium leads to an increased renal filtered load of calcium and increased urine calcium excretion (99). This may also indicate that females (both humans and other mammals) take in more calcium than needed during pregnancy, with the kidneys excreting the excess.

1.2.2 During lactation

At pregnancy, the calcium balance may be neutral or slightly negative; during lactation, a net loss of calcium occurs to provide sufficient calcium for milk production. The daily calcium loss in women normally ranges from 280 to 400 mg, sometimes reaching 1000 mg (99). In order to maintain maternal calcium homeostasis during lactation, different physiological strategies are employed during pregnancy.

Unlike a possible modest increase in bone metabolism during pregnancy, bone resorption is markedly increased during lactation in order to provide the needed calcium for milk (99). This leads to a net bone loss of 5 – 10% over 3 – 6 months in humans and 25 – 30% over 3 weeks in normal rodents. As discussed earlier, PTH stimulates osteoclast-mediated bone resorption, but PTH normally becomes suppressed during lactation and does not drive bone resorption. Even without PTH, women and rodents lactate normally (107). The

circulating PTHrP concentration goes up during lactation and appears to be produced by mammary tissues, where tissue and milk levels of PTHrP are 1,000 – 100,000 times greater in concentration than in blood (108). Supporting evidence that PTHrP is needed for bone resorption during lactation includes the fact that a conditional knockout of PTHrP from mammary tissue at the onset of lactation causes less bone to be resorbed (108). In addition, human studies of hypoparathyroidism show that calcium and bone metabolism returns to normal during lactation. PTHrP is likely acting on the PTHR at the surface of osteoblasts to increase osteoclast differentiation by RANKL/RANK/OPG pathway. Also during lactation, estrogen is inhibited by prolactin and by direct actions of suckling to inhibit GnRH. Low estrogen is known to increase bone resorption by increasing the ratio of RANKL to OPG. Thus during lactation, the effects of low estrogen and high PTHrP combine to stimulate more bone resorption than either alone should cause.

Some studies have found that PTH may not be suppressed during lactation in humans, rats and certain strains of mice. This has been reported in women from Asia and Africa who have habitually low intakes of calcium or high intakes of phytate, which blocks intestinal calcium absorption (109). In rodents, a high litter size or a low calcium intake will induce a compensatory rise in PTH. And so in rodents both PTHrP and PTH may be needed to ensure that sufficient calcium is provided to meet the needs of the suckling pups without causing hypocalcemia in the mother.

The kidneys also participate in the maintenance of the maternal calcium supply during lactation. Calcium is actively reabsorbed such that the urine calcium falls to low levels. Since PTH is normally low during lactation, PTHrP is likely enhances tubular calcium reabsorption by mimicking the renal actions of PTH (110, 111).

Quite different from the increased intestinal calcium absorption during pregnancy, intestinal calcium absorption decreases during lactation to non-pregnant levels in humans (112, 113). Even though maternal calcium intake may be increased during this period, there is no difference in the rate of calcium absorption between lactating and non-pregnant women. This change may be in response to the fall of calcitriol to normal levels during lactation as well as the reversal of estrogen and placental lactogen levels (114, 115). In contrast to humans, rats maintain an increased calcitriol level during lactation and increased intestinal calcium absorption (116). Relative low body weight and large litter size (high demand for milk) may make rats develop this adaptation to support calcium homeostasis during lactation. Mice appear to similarly have elevated calcitriol and likely increased intestinal calcium absorption during pregnancy (105).

1.2.3 During recovery after lactation

The bone loss resulting from lactation is fully and quickly reversed afterwards with recovery of BMC back to the pre-pregnant level or higher (77, 107, 117). The recovery process usually takes 6 – 12 months and 10 – 20 days in humans and mice, respectively. So far the mechanisms underlying post-weaning recovery are still unclear. Understanding

these mechanisms will not only increase our knowledge of human physiology but may also provide novel ways of stimulating bone formation to treat osteoporosis.

Up to now our lab has confirmed that loss of PTH, VDR, calcitonin, or osteoblast-derived PTHrP has no effect on bone recovery after lactation (104, 118). Estrodiol levels are suppressed during lactation and return to normal afterward, and this might stimulate bone recovery. However, estradiol is not a potent stimulator of osteoblast functions, and experimental evidence in humans and rodents suggests that estradiol is not responsible for rapid bone recovery after weaning. Further research to understand the mechanism underlying post-weaning recovery is needed.

1.3 Animal model: CTR gene (*Ctr*) heterozygous mice

This study uses mice in which the gene encoding the CTR (*Ctr*) has been ablated. *Ctr* heterozygous mice are maintained on the C57BL/6J inbred strain (C57), which is widely used in laboratory research. *Ctr* is located at chromosome 6 in C57 mice. Exon 6 and Exon 7 of *Ctr* were ablated by insertion of neomycin to block all isoforms of CTR in C57/BL6J mice, thus blocking the *Ctr* expression. Three genotypes result from mating heterozygous males and females together: wildtype with both normal *Ctr* alleles, heterozygous (HET or *Ctr*^{+/−}) with one normal *Ctr* allele and one *Ctr* allele knocked out, and null with both *Ctr* alleles knocked out (*Ctr*^{−/−}). Unfortunately, most *Ctr* null mice die mid-gestation due to unknown reasons, and very few studies have been done on them (119). A few null mice have survived in our laboratory, but very infrequently.

Heterozygous mice ($Ctr^{+/-}$) have been studied as adults. They are phenotypically normal, fertile, and have normal life spans. *Ctr* expression was found to be decreased by twofold in osteoclasts obtained from $Ctr^{+/-}$ mice (19). *C57 Ctr^{+/-}* mice have also been found to have increased bone mass due to promoted bone formation (19), but the mechanism by which partial loss of calcitonin's actions would lead to increased bone mass is unknown.

1.4 Project description

Previous studies in our lab have shown that calcitonin protects against excessive bone resorption during lactation since calcitonin null mice ($Cr^{-/-}$) lost twice as much bone as WT sisters (77). CTR is known to be expressed by osteoclasts, mammary tissue, and pituitary. However, we do not know which of these three CTR sites are required for calcitonin's actions during lactation: in bone, calcitonin directly suppresses osteoclast-mediated resorption; in mammary tissue, it may play a role in regulating calcium pumping or PTHrP expression, since in its absence both milk calcium and PTHrP expression increased; in the pituitary gland, calcitonin appears to suppress prolactin, and so its absence during lactation could induce higher prolactin levels, which would cause both more profound estrogen deficiency and greater stimulation of PTHrP expression.

The original purpose of my project was to determine whether global loss of *Ctr* leads to the same phenotype as loss of calcitonin. If so, this would enable more targeted studies to address which tissue (osteoclasts at bone tissue, mammary tissue, or pituitary) and

through which mechanisms the calcitonin-CTR interaction regulates calcium and bone metabolism during lactation; however, due to most *Ctr* null mice dying *in utero*, I have had to use *Ctr*^{+/-} mice instead. Since previous investigators showed *Ctr* to be down regulated 2-fold in *Ctr*^{+/-} mice, this model seemed appropriate to study as a haploinsufficient model of CTR signaling. In this project, the BMC phenotype was determined first in both C57 WT and *Ctr*^{+/-} mice throughout the reproductive cycle, and then the potential factors contributing to it were investigated.

2 Materials and methods

2.1 Animal husbandry

Ctr^{+/-} mice maintained in the C57 background were kindly provided by Dr. Galson (Department of Medicine, University of Pittsburg, Pittsburgh, PA, USA). They were raised on a regular laboratory mouse diet (1% calcium, 0.75% phosphorus, 22% protein, 5% fat) and maintained in the Animal Care Facility at Memorial University of Newfoundland. The animal holding room is set on a light timer of *on* at 8 a.m. and *off* at 8 p.m. for a total of 12 hours of light and 12 hours of dark per 24 hours. Both female and male mice were weaned when three weeks (wk) old. Male and female mice were separated into different cages with a maximum of four mice per cage. After 10 wk of age, when mice reach a plateau in bone mass and are sexually mature, one pair of virgin female mice (one WT, one *Ctr^{+/-}*) within the same litter was randomly selected to mate with the same male mouse from a different mother. The next morning, the male and female mice were separated and the female mice were checked for a mucus plug, which indicates that mating has occurred. Female mice with mucus plugs were put into separate cages, and the day was marked as Day 0.5 of pregnancy. Pregnancy proceeded normally, and the pups were allowed to be born and nursed normally. At Day 21 of lactation, pups were manually weaned from their mother. To exclude the possibility that the number of pups could affect the BMC phenotype of WT and *Ctr^{+/-}* mice, litter size was recorded. No litters were included where the mother had less than 5 or more than 10 pups. All mouse experiments were approved by the Institutional Animal Care Committee of Memorial University of Newfoundland.

The reproductive cycles of WT and *Ctrl*^{+/+} mice were consistent. After 7 – 10 days (d) of pre-pregnancy baseline, a full reproductive cycle lasted about 61 d. This included gestation of 19 d, lactation of 21 d, and 3 wk of recovery after lactation. At the end of lactation, the litter size of experimental dams was recorded.

2.2 Experimental time points and design

All experiments involved comparisons between *Ctrl*^{+/+} and WT mice at the following time points. During a 7 – 10 d interval after 10 wk of age and before mating, experimental samples were collected twice and marked as baseline 1 and baseline 2. Gestation lasted 19 d, and so at Day 18.5 of pregnancy, experimental samples were collected and marked as late pregnancy. The day when pups were delivered was considered Day 1 of lactation. Experimental samples collected at Day 7 of lactation were marked early lactation, and those collected at Day 21 of lactation were marked late lactation. After weaning (Day 21 of lactation), samples were collected at weekly intervals (the end of each recovery week) and marked recovery 1, recovery 2, and recovery 3, respectively. A brief description of experimental samples collected at each time point, and the application of those samples, are shown in Figure 2. Detailed experimental procedure is described in the following sections.

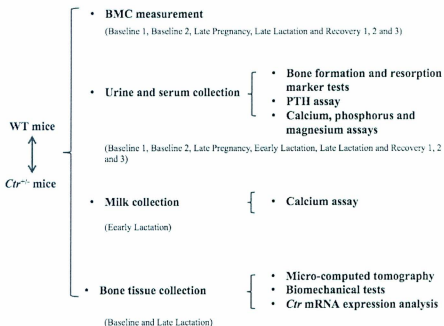


Figure 2: Experimental design. Experiments in my master's project are briefly described here. The time points of samples collected for each experiment are shown in parentheses.

2.3 Genotyping

Polymerase chain reaction (PCR) was carried out to determine the genotype of pups from HET × HET mating. The whole process included tagging and tailing, Deoxyribonucleic Acid (DNA) extraction, PCR, and gel electrophoresis.

2.3.1 Tagging and tailing

Mice were briefly anaesthetized with isoflurane. During the 10 – 15 seconds (s) of unconsciousness, an ear tag with a unique number was applied to the right ear. Right after the tagging, 1 cm of tail was cut by sterile razor blade and put into a sterile micro-centrifuge tube containing 0.5 ml lysis buffer [100 mM Tris HCL, pH 8.0; 500 mM ethylenediaminetetraacetic acid (EDTA), pH 8.0; 0.2% sodium dodecyl sulfate (SDS); 200 mM sodium chloride (NaCl); 100 µg/ml proteinase K (Invitrogen)]. The tails were digested at 55°C overnight.

2.3.2 DNA extraction

The morning after tagging and tailing, micro-centrifuge tubes containing digested tails were shaken by hand for 2 to 3 min, and then spun on a centrifuge (IEC Micromax) for 10 min at 15,000 revolutions per minute (rpm) to precipitate hair. The supernatant was poured into fresh tubes containing 0.5 ml isopropanol (HPLC grade, Fisher Scientific) and then tubes were inverted to precipitate DNA. The DNA pellet was physically picked out with small pipette tips and put into a fresh eppendorf tubes containing 0.5 ml water. The tubes were shaken by hand for 5 min to dissolve DNA into a viscous solution. In the

fumehood, 0.5 ml well-mixed phenol/chloroform/isoamyl alcohol (25:24:1) (Fisher Scientific) at 4°C was added to the tubes. The tubes were shaken by hand for 1 min until the solution became turbid and milky, and then tubes were centrifuged for 2 min at 15,000 rpm. In the fumehood, the supernatant of each tube was carefully pipetted off and placed in a fresh eppendorf tube. One ml of Ethanol sodium acetate (EtOH:NaOAc) (25:1) solution at -20°C was added to the supernatant. Tubes were inverted several times until DNA came out of the solution. Tubes were centrifuged for 10 min at 15,000 rpm. The supernatant was discarded and 1 ml 70% EtOH was added to wash the DNA pellet. Tubes were spun for 10 min at 15,000 rpm. EtOH was poured off and the rest was pipetted off. The DNA pellet was air dried for 2 h and then resuspended with 50 µL TE buffer (10 mM Tris, 1 mM EDTA, pH 8.0). The DNA sample was stored at 4 °C until further use.

2.3.3 PCR

PCR was carried out on the DNA collected from mice tails. In order to distinguish *Ptr*^{+/+} from WT mice, a 4-primer system was used, including one pair for *Ptr* and one pair for neomycin cassette (Neo). Primer sequences are as follows: *Ptr*-Forward: 5'- CAG CCT GTA AGC TTT CAG CCA -3', *Ptr*-Reverse: 5'- ATT CTT ATC CAA TAC AGA GAT T -3', Product = 229 bp; Neo-Forward: 5'- ATG CCG CCG TGT TCC -3', Neo-Reverse: 5'- GCC CCT GAT GCT CTT CGT -3', Product = 400 bp.

Each PCR mix (49 µL) was made with the following ingredients: 1× PCR Run Buffer

(20mM Tris-HCl, 50 mM Potassium chloride (KCl)) (Invitrogen), Deoxyribonucleotide triphosphates (dNTPs) (0.2 mM Deoxyadenosine-5'-triphosphate (dATP) : 0.2 mM Deoxythymidine triphosphate (dTTP) : 0.2 mM Deoxycytidine triphosphate (dCTP) : 0.2 mM Deoxyguanosine triphosphate (dGTP): H₂O = 1 : 1 : 1 : 1 : 1) (Invitrogen), 0.4 mM primers (*Ctr*-Forward, *Ctr*-Reverse, *Neo*-Forward, *Neo*-Reverse), 50mM MgCl₂, 1 U Taq DNA Polymerase (0.02 U/ μ L) (Invitrogen) and deionized water. 1.5 μ L of DNA sample was added into the solution in each PCR tube. PCR tubes were put on Peltier Thermal Cycler-Dual Alpha Blocks (PT-200 DNA Engine Thermal Cycler) for reactions.

The PCR cycling program was as follows: Step 1: 94 °C for 2 minutes for initial denaturation; Step 2: 94 °C for 40 seconds for denaturation; Step 3: 54 °C for 30 seconds for annealing; Step 4: 72 °C for 40 seconds for extension; Step 5: back to Step 2 and repeat 35 times; and Step 6: 4 °C indefinitely.

2.3.4 Gel electrophoresis

Horizontal gel electrophoresis was used to separate and display the PCR products. The gel was made with the following ingredients: 10 ml 10 \times Tris-acetate-EDTA buffer (0.12 M EDTA, 0.40 M Tris, 11.5% Glacial Acetic Acid, pH 8.0), 90 ml deionized water, 1.2% agarose (1.2 g) (Invitrogen) and 10 μ L SYBR Safe DNA Gel Stain (Invitrogen). Agarose powder was added into the TAE buffer solution and then dissolved in the microwave (2 min). SYBR gel stain was added to the solution, and all the ingredients were well mixed. The solution was poured into the gel mold and allowed to solidify. The gel running buffer

was made as follows: 70 ml 10× TAE buffer was diluted by 630 ml deionized water to prepare 1× TAE working buffer.

Orange G (Sigma, United States) was used as gel loading dye. It was made with 100 ml 10× TAE, 500 mg Orange G, and 50 ml 100% Glycerol. 2 μ L of Orange G was added to the PCR product and mixed well. 15 μ L of PCR product and the loading dye mix was injected into each well of the gel. 200 V was applied across the gel in running buffer for 20 min.

The gel was imaged under UV excitation with digital photography (Gel Logic 100, Mandel). The results were read using Kodak MI software. A single 229 bp band of *Ctrl* indicated WT mice, a single 400 bp band of Neo cassette indicated null mice, and both 229 bp and 400 bp bands of *Ctrl* and Neo cassette indicated heterozygous (*Ctrl*^{+/-}) mice.

2.4 BMC measurement

BMC was measured by Lunar Piximus2 dual-energy X-ray (DXA) bone densitometer (General Electric) to investigate BMC pattern changes during the reproductive period of both *Ctrl*^{+/-} and WT mice. The densitometer was calibrated using a Phantom with 11.9% fat and 0.063 g/cm² BMD each day. The deviation of both fat and BMD for quality control was < 2%. The BMC value of each experimental mouse was measured at baseline 1, baseline 2, late pregnancy, late lactation, and recovery 1, 2, and 3. Prior to the DXA scanning, mice were anaesthetized by an i.p. injection of 40 μ L of 83.3 mg/ml Ketamine

and 3.3 mg/ml Xylazine. The anaesthetized mice were placed onto the holding trays and then put into the scanning window on the densitometer for whole body scanning. After the scanning was completed, dams were laid in a warm place until awake and then were returned to pups. The scan image was adjusted to exclude the head. The main value obtained was whole body BMC (excluding the head). The BMC values of the lumbar spine (L1-L6) and left tibia were calculated from the whole body scanning results of the software, which enabled these regions of interest to be highlighted. In addition to analyzing the absolute value of BMC, the values obtained during the reproductive cycle of each mouse were expressed as a percentage change from the pre-pregnancy baseline value.

2.5 Urine and serum collection

Urine and serum were collected at baseline 1, baseline 2, late pregnancy, early lactation, late lactation and recovery 1, 2, and 3. Experimental mice were placed in clean cages containing one mouse each. The mice normally void promptly. Urine was immediately collected into small sterile centrifuge tubes by pipette and stored in the freezer at -20 °C. Serum collection was conducted after each BMC measurement while the mice were still anesthetized. The end of the mouse tails was cut using a sterile razor blade. Blood was collected into small centrifuge tube while applying light pressure on the tail. The collected blood was placed at room temperature for at least half an hour and then centrifuged for 8-9 minutes at 14,000 rpm. Serum was separated as the top layer (supernatant liquid) from the whole blood. Serum was stored at -20 °C.

2.6 Milk collection

Milk was collected from experimental dams at early lactation for milk protein and calcium analyses. Pups were separated from mothers 1 h before milk collection. The dams were injected (i.p.) with 40 μ L of 83.3 mg/ml Ketamine and 3.3 mg/ml Xylazine, and 1 IU of Oxytocin (100 μ L of solution). Oxytocin stimulates milk let down and ejection. When the mice were under anesthesia, mice were placed supine (abdomen with an upward exposure), and hair was pushed down to expose the nipples. The mammary gland was squeezed from the root to the top by hand, and capillary tubes were used to collect milk coming out from the nipples. An average of 60 μ L of milk could be collected from one mouse. The collected milk was transferred from capillary tubes to plastic centrifuge tubes and stored at -20 °C.

2.7 Bone tissue collection

Bone tissues, including forelimbs, lumbar spines, and tibias, were collected from all mice. Tibias were collected at pre-pregnancy baseline for *Ctrl* expression analysis. Lumbar spines and tibias were collected at late lactation for micro-computed tomography and biomechanical tests. Mice were euthanized by cervical dislocation. Tibias for *Ctrl* expression analysis were harvested immediately. Once flesh attached to the tibias was removed by forceps, the tibias were snap-frozen in liquid nitrogen and then stored at -80 °C freezer. Lumbar spines (L1 – L6) and tibias for biomechanical tests were harvested by the same methods, but stored at -20 °C.

2.8 Serum and urine total calcium measurement

The total calcium assay is based on the principle that Arsenazo III reacts with calcium to form Arsenazo III-calcium complex, which displays blue-purple color. The color has maximal absorbance at a wavelength of 650 nm and is directly proportional to the concentration of total calcium. Serum and urine samples at baseline (pooled by baseline 1 and baseline 2 samples), late pregnancy, late lactation and recovery 1, 2, and 3 were tested. Prior to the measurement, urine was diluted in saline by a factor of 10. Samples were measured in duplicate according to the procedure in the kit (Genzyme Diagnostics, Reference Number: 140-20). The absorbance was read at 650 nm in a spectrophotometer (Ultraspec 2000, Pharmacia Biotech). The final results of urine total calcium were expressed as urine total calcium concentrations normalized to urine creatinine concentrations (mmol Ca/mmol Creatinine). Deionized water was used as a blank.

2.9 Serum and urine inorganic phosphorus measurement

This assay was based on the principle that inorganic phosphorus reacts with ammonium molybdate in the presence of sulfuric acid to produce unreduced phosphomolybdate complex. The increase in absorbance at a wavelength of 340 nm is directly proportional to the concentration of inorganic phosphorus in the samples. Serum and urine samples at baseline (pooled by baseline 1 and baseline 2 samples), late pregnancy, late lactation and recovery 1, 2, and 3 were measured. Prior to the assay, urine was diluted in saline by a factor of 10. Experiments followed the instructions in the kit (Genzyme Diagnostics P.E.I. Inc., Catalogue number: 117-10) in duplicate. The absorbance was read in a

spectrophotometer (Ultrospec 2000, Pharmacia Biotech) at 340 nm. The final results of urine phosphorus were expressed as phosphorus concentrations normalized to urine creatinine concentrations (mmol P/mmol creatinine). Deionized water was used as a blank.

2.10 Serum and urine magnesium measurement

Serum and urine magnesium concentrations were tested. This assay was based on the principle that xylydyl blue-1 reacts with ionized magnesium to form Mg-xylydyl blue complex (red). The increase in the absorbance at 520 nm wavelength is directly proportional to the concentration of magnesium in the samples as a result of the red complex formed. Serum and urine samples at baseline (pooled by baseline 1 and baseline 2 samples), late pregnancy, late lactation and recovery 1, 2, and 3 were tested. Prior to the assay, urine samples were diluted in saline by a factor of 10. Experiments were conducted in duplicate according to the procedure in the kit (Diagnostic Chemicals Limited, Catalogue number: 125-12). Absorbance was measured at 520 nm in a spectrophotometer (Ultrospec 2000, Pharmacia Biotech). The final results of urine magnesium were normalized to urine creatinine concentrations (mmol Mg/mmol creatinine). Deionized water was used as a blank.

2.11 Urine creatinine measurement

Creatinine was measured to normalize the values of all urinary metabolites. The assay was based on the principle that in an alkaline environment, creatinine reacts with alkaline

picrate to produce creatinine-picrate Janousky complex. The amount of increase in absorbance at a wavelength of 510 nm is directly proportional to the concentration of creatinine in the sample. Urine samples at Baseline (pooled by baseline 1 and baseline 2 samples), late pregnancy, early lactation, late lactation and recovery 1, 2, and 3 were tested. A dilution factor of 10 was used. Experiments followed the procedure in the kit (Diagnostic Chemicals Limited, Catalogue number: 221-30) in duplicate. The results (mmol) were read at 510 nm in a spectrophotometer (Ultrospec 2000, Pharmacia Biotech). Deionized water was used as a blank.

2.12 Serum procollagen type I N-terminal propeptide (PINP) assay

PINP is a bone formation marker. The synthesis of type I collagen, which is the major organic component in bone matrix, is an essential step in bone formation. During formation of the collagen, propeptides are derived from both N- and C-terminal ends of the procollagen molecule. These propeptides are released into the circulation, making the detection of such propeptides available through enzyme immunoassay (EIA). Therefore, the concentration of PINP in serum can reflect the activity of bone formation. A PINP kit (Immunodiagnostic Systems Holdings plc, Reference number: AC-33F1) applies competitive EIA methodology using a polyclonal rabbit anti-PINP antibody. Serum samples at baseline (pooled by baseline 1 and baseline 2 samples), late pregnancy, late lactation and recovery 1, 2, and 3 were measured. Experiments were carried out according to the methods described in the kit in duplicate. Results were read at 450 nm (reference 650 nm) in a microplate reader (Model 3550, Bio-Rad).

2.13 Urine deoxypyridinoline (DPD) assay

DPD is a bone resorption marker. Type 1 collagen in bone matrix is crosslinked by pyridinoline (PYD) and DPD, both of which can provide rigidity and strength. DPD is derived from the enzymatic reaction of lysyl oxidase on the amino acid lysine. DPD is released from bone matrix into the circulation while bone is resorbed and excreted into urine without any effect from the diet. The process makes DPD detection available by EIA. Therefore, the DPD concentration in urine can reflect the extent of bone resorption *in vivo*. Urine samples at baseline (pooled by baseline 1 and baseline 2 samples), late pregnancy, early lactation, late lactation and recovery 1 were compared. DPD EIA kit (MicroVue Quidel, Reference number: 8007) is a competitive EIA utilizing monoclonal anti-DPD antibody that was used by duplicate according to manufacture's instructions. Results were read at 405 nm in a microplate reader (Model 3550, Bio-Rad). The final results were expressed as DPD concentrations normalized to urine creatinine concentrations (mmol DPD/mmol Creatinine).

2.14 Serum PTH assay

PTH plays an essential role in maintaining calcium homeostasis *in vivo*. A PTH kit (Immutopics, Catalogue number: 60-2300) is specific for the intact 84 amino acids of PTH. It applies two-site enzyme-linked immunosorbent assay (ELISA) methodology to determine serum PTH concentration. PTH is captured by anti-mouse PTH antibody (second antibody) anchored at the surface of the well. Biotin-horseradish peroxidase (HRP) system is used to detect the concentration of PTH by using HRP-labeled anti-

mouse PTH antibody (first antibody). Serum samples at baseline (pooled by baseline 1 and baseline 2 samples), late pregnancy, late lactation, and recovery 1 were used to detect PTH concentration during reproductive period. Experiments followed the procedure in the kit in duplicate. Results were read at 450 nm in a microplate reader (Model 3550, Bio-Rad).

2.15 Milk protein measurement

Since much of the calcium in milk is bound to milk proteins, the protein level in milk was assayed to normalize milk calcium concentration. The principle of milk protein measurement was based on the biuret reaction: Cu^{2+} is reduced to Cu^{1+} by protein in an alkaline medium, forming Cu^{1+} -protein complex, and the Cu^{1+} level can be colorimetrically detected by using bicinchoninic acid. The absorbance of Cu^{1+} in the complex is directly proportional to protein content (20-2000 $\mu\text{g}/\text{ml}$) at 562 nm wavelength. Milk collected at early lactation was used, and the measurement followed the procedure in the kit (Pierce BCA Protein Assay Kit, Thermo Scientific) by triplicate. Results were read at 562nm in a microplate reader (Polarstar Optima, BMG).

2.16 Milk calcium measurement

Milk calcium content was measured by flame atomic absorption spectroscopy (Perkin-Elmer 2380 Atomic Absorption Spectrometer). The principle is that electrons of calcium atoms are promoted to a higher orbit by the flame, thus absorbing radiation of calcium-specific wavelength. By comparing radiation flux without and with calcium-containing

samples, calcium concentration is calculated based on Beer-Lambert Law by a calculator in the machine. Milk was brought to room temperature and then diluted by a dilution factor of 200 (5 μ L milk in 995 μ L nitric acid). Low (2.5 μ g/ml), medium (7.5 μ g/ml), and high (15 μ g/ml) calcium standards were made by calcium reference standard solution (Fisher Scientific) and nitric acid. Measurement of standards and milk samples followed the manual of the atomic absorption spectrometer. Milk samples were tested in triplicate.

2.17 Micro-computed tomography (μ CT)

Frozen lumbar spines were fixed in formalin buffer and sent to the Centre for Bone and Periodontal Research at McGill University for μ CT. It was performed using a high resolution μ CT scanner (SkyScan-1072, Aartselaar, Belgium). The largest lumbar vertebrae in each sample tube were selected for analysis. The vertebrae were wrapped with Parafilm to prevent dehydration and then scanned at a source power of 45 kV/222 μ A and spatial resolution of 5.63 μ m/pixel. The rotation was set at 0.9 degrees/step for 180 degrees and the exposure time was set at 2.8 seconds/step. Images were taken by X-Ray CCD-camera based on a cooled 12-bit CCD-sensor of 1024x1024 pixels. 2D cross-section images from μ CT scans were used to construct and calculate the 3D architectural parameters for the trabecular bones in the lumbar including mean trabecular thickness, mean trabecular spacing, total volume, anisotropy, volume fraction (%), volume (mm^3), surface (mm^2), surface/volume (%) and structure model index.

2.18 Biomechanical tests

2.18.1 3-point bend test

3-point bend (3PB) tests were carried out to measure the differences of cortical bone strength between WT and *Ctrl*^{+/+} mice throughout the reproductive cycle. Tibias for 3PB tests were collected from WT and *Ctrl*^{+/+} mice at both baseline and late lactation. They were put into PBS and then thawed at room temperature for at least 2 h prior to analysis. The tests were performed by a single-column Instron Series 3340 electromechanical test instrument (Instron, Norwood, MA, USA) together with the Instron Series IX/s software package. Tibias with the same length were carefully placed on the platform with each end fixed. A load cell of 10 N was set 1cm above the tibia midshaft. Once the analysis began, the cross-head of the load cell descended at 10mm/minute until the tibia was broken. Parameters including maximum load, displacement (μm), maximum strain (gf/mm^2), maximum strain (%), and slope (gf/mm) were recorded and displayed by the software.

2.18.2 Reference point indentation test

The reference point indentation (RPI) test is an alternative method of detecting cortical bone strength. The principle is that the test probe, which is shielded by the outer reference probe from surrounding soft tissues, hits the bone surface to make a displacement relative to the reference point set by the outer reference probe. The value of the displacement [Indentation distance increase (μm)] is used as an indicator of cortical bone strength. The bone surface isn't permanently deformed by this procedure. Tibias and vertebrae from WT at baseline stage and late lactation stage were sent to Active Life Scientific, Inc.

(Santa Barbara, CA, USA) for the RPI test. Unfortunately the company declined to test the *Ptr*^{+/-} samples as well, saying that they could only do proof-of-principle tests on the WT samples and not a collaborative analysis of WT vs. *Ptr*^{+/-} samples.

2.19 *Ptr* gene expression analysis

Ptr expression at bone tissue was tested to determine the effect of haploinsufficiency on *Ptr*^{+/-} mice. The whole process included ribonucleic acid extraction, cDNA synthesis and real-time quantitative RT-PCR.

2.19.1 RNA extraction

Total RNA was extracted from both left and right tibias of female mice using the RNeasy Midi Kit (Qiagen). Experimental steps followed the protocol in the kit. After extraction, RNA concentration and quality were measured on the 2100 Bioanalyzer platform (Agilent Technologies).

2.19.2 cDNA synthesis

Two µg of mouse tibia RNA samples were used for cDNA synthesis by Superscript III First-strand Synthesis System (Invitrogen). The experimental procedure followed the protocol in the kit. The synthesis program was as follows: Step 1: 25 °C for 10 min; Step 2: 37 °C for 2 h; Step 3: 85 °C for 5 min; Step 4: 4 °C indefinitely.

2.19.3 Real-time quantitative RT-PCR

Real-time quantitative RT-PCR was conducted using Taqman® Universal PCR Master Mix (Applied Biosystems) on the ViiA™ Real-time PCR System (Applied Biosystems). A minor groove binder (MGB) probe with a Fluorescent reporter dye 6-carboxylfluoresceine (FAM) reporter dye at the 5' end and a non-fluorescent quencher at the 3' end were used in the assay. When targeted cDNA was amplified, the MGB probe was digested by DNA polymerase and the FAM reporter dye was released. Fluorescence from free FAM reporter dye was detected by the real-time PCR system. The intensity of fluorescence was directed to the concentration of targeted cDNA within proper range. *Ctr* primers were pre-designed by Applied Biosystems (Mm00432271_m1). The experiment followed the protocol in the kit. All samples were tested in triplicate and threshold cycle value was used as indicator of gene expression. GAPDH was used as endogenous control.

The real-time quantitative running program was as follows: Step 1: 50 °C for 2 min for Uracil-N-glycosylase (UNG) incubation; Step 2: 95 °C for 20 s for polymerase activation; Step 3: 95 °C for 1 s to denature; Step 4: 60 °C for 20 s for annealing; Step 5: Back to step 3 and repeat 40 times.

2.20 Statistical analysis

SYSTAT 5.2.1 for Macintosh (SYSTAT Inc, Evanston, IL, USA) was used for data analysis. Significant differences among means were calculated by analysis of variance (ANOVA), and Tukey's test was carried out to determine which pair(s) of mean(s) was

(were) significantly different. Real-time RT-PCR results were analyzed by a $2^{-\Delta\Delta C_T}$ method. All experimental results were expressed as the form of mean \pm standard error (SE). Any significant differences were marked in the graphs. The number of samples studied was indicated in parentheses in the graphs.

According to previous studies in our lab, the minimum sample size for each group to find significant differences is 5 mice for BMC measurement. P1NP, DPD, PTH, and serum and urine mineral assays require at least 5 samples of each group. Collaborators have advised that the 3-point bend test needs 15 samples of each group for the most reliability, but such a high number of samples were not practical for this study.

3 Results

3.1 Genotyping

In order to distinguish *Ctr^{+/+}* and WT female mice, DNA samples were extracted from the tails to genotype by PCR. Consistent with previous studies, no CTR null mice were observed from C57 HET \times HET mating due to their death in mid-gestation. Thus, in the following experiments, I compared WT mice to *Ctr^{+/+}* mice. An example of genotyping results is shown in Figure 3.

3.2 Litter size

WT and *Ctr^{+/+}* mice had the same mean litter size, with 8 ± 0 in WT and 8 ± 1 in *Ctr^{+/+}* respectively. Results are shown in Figure 4.

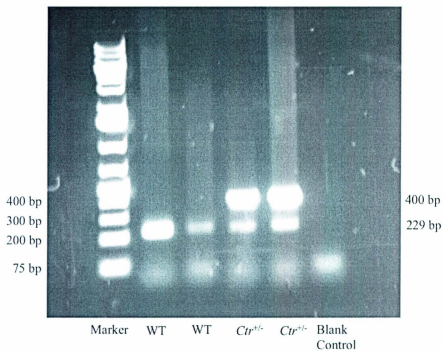


Figure 3: Example of genotyping results. A single band at 229bp indicated the genotype as WT, while bands at both 229 bp and 400bp indicated the genotype as *Ctrl*^{+/-}. A single band at 400 bp would indicate a null mouse, but none were found during the whole project. A blank Control was used in PCR.

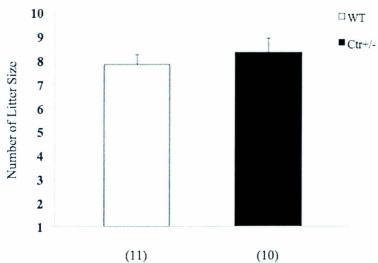


Figure 4: Litter sizes in WT and $Ctr^{+/-}$ mice at Late Lactation. The numbers of pups in both WT and $Ctr^{+/-}$ mice were counted at Late Lactation. No significant difference of litter size was found between WT and $Ctr^{+/-}$ female mice.

3.3 BMC measurement

At pre-pregnancy baseline stage, the BMC of WT and *Ctrl*^{+/-} mice was not different (0.501 ± 0.021 and 0.520 ± 0.018 , respectively) (Figure 5).

Relative changes of whole body BMC (largely cortical bone) of both WT and *Ctrl*^{+/-} mice throughout the reproductive period are shown in Figure 6. Both genotypes gained a similar percentage of bone relative to baseline during pregnancy ($7.4 \% \pm 3.4 \%$ in WT and $7.7 \% \pm 3.9 \%$ in *Ctrl*^{+/-}). During lactation, WT and *Ctrl*^{+/-} mice each lost about 18% of BMC, falling to $-10.7 \% \pm 3.4 \%$ BMC and $-10.6 \% \pm 2.0 \%$ BMC relative to baseline, respectively, and these values were significantly different from late pregnancy ($p < 0.01$). After weaning, both groups recovered to a mean value above Baseline, achieving a $4.6 \% \pm 3.8 \%$ increase in WT and $2.9 \% \pm 3.1 \%$ increase in *Ctrl*^{+/-}, but these were not significantly different from baseline. No significantly different changes in whole body BMC pattern between WT and *Ctrl*^{+/-} were observed throughout the reproductive period.

The lumbar spine contains much more trabecular bone and showed a different response during the reproductive period as shown in Figure 7. For both genotypes, the BMC declined by the end of pregnancy ($-11.3 \% \pm 3.2 \%$ of WT vs. $-10.4 \% \pm 4.0 \%$ of *Ctrl*^{+/-}). The BMC declined even further during lactation to a trough value of $-17.1 \% \pm 3.0 \%$ BMC in WT and $-19.2 \% \pm 2.7 \%$ in *Ctrl*^{+/-}. Both WT and *Ctrl*^{+/-} recovered back to baseline level within 14 d of weaning with no significant difference when compared with baseline level. WT and *Ctrl*^{+/-} mice did not show any significant differences in lumbar spine BMC at any time point during the reproductive cycle.

The hind limb represents an intermediate mix of cortical and trabecular bone, and its response to the reproductive periods differed from the whole body and spine. Relative BMC changes at this site are shown in Figure 8. WT and *Ctr^{+/-}* mice gained $20.3\% \pm 3.8\%$ and $20.0\% \pm 6.3\%$ respectively by late pregnancy, and the BMC significantly decreased during lactation by about 26% to reach trough values of $-6.0\% \pm 3.5\%$ and $-7.4\% \pm 2.6\%$ respectively ($p < 0.0002$). After weaning, the BMC of WT and *Ctr^{+/-}* increased above baseline to $6.4\% \pm 3.7\%$ and $4.2\% \pm 3.8\%$, respectively, but these were not significantly higher than baseline. There were no significant differences between WT and *Ctr^{+/-}* throughout the reproductive period.

3.4 Absolute BMC values

For clarity, the absolute whole body BMC values of WT and *Ctr^{+/-}* mice during the reproductive period are shown in Figure 9. BMC of WT declined from 0.501 ± 0.020 at baseline to 0.442 ± 0.010 at late lactation ($p < 0.05$) and BMC of *Ctr^{+/-}* decreased from 0.520 ± 0.018 at baseline to 0.462 ± 0.013 at late lactation ($p < 0.05$). During post-weaning recovery, the BMC of both returned to baseline level. No significant differences between WT and *Ctr^{+/-}* were found at any time point.

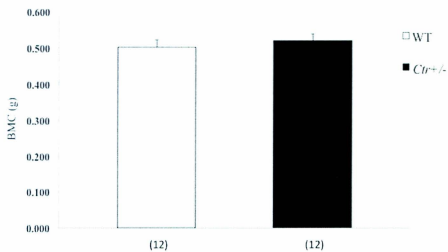


Figure 5: BMC (g) in WT and $Ctr^{+/-}$ mice at Baseline. At baseline stage, BMC was measured by DXA and showed no difference between WT and $Ctr^{+/-}$.

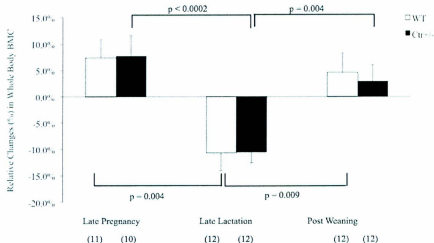


Figure 6: Whole body BMC changes relative to BMC at Baseline throughout reproductive period. In general, BMC increased during pregnancy, declined during lactation, and returned to slightly above baseline after weaning. Although the BMC excursions were significant for each genotype, no significant differences were observed between WT and *Cr*^{+/-} mice at any time point.

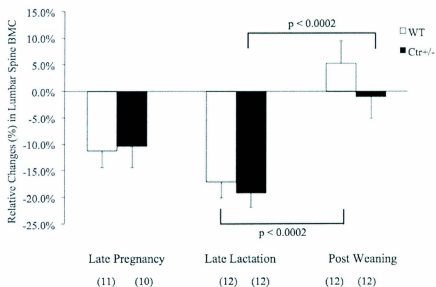


Figure 7: Lumbar spine BMC changes relative to BMC at Baseline throughout reproductive period. The lumbar spine BMC declined in both genotypes during pregnancy and even further during lactation, before recovering after weaning. There were no significant differences between WT and *Ctrl*^{+/-} mice at any time point.

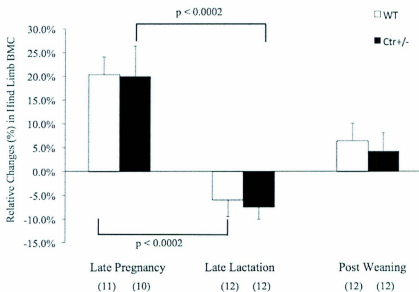


Figure 8: Hind limb BMC changes relative to BMC at Baseline during reproductive period. The hind limb showed the greatest relative increase in BMC during pregnancy, followed by a decline during lactation, and an increase to slightly above Baseline after weaning. No significant differences were seen between WT and *Ctrl^{+/-}* mice.

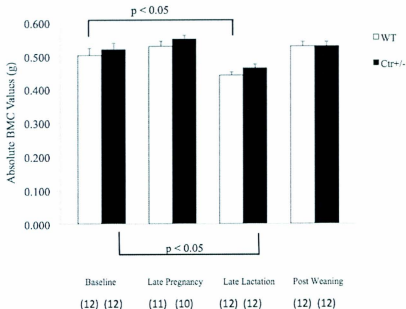


Figure 9: Absolute whole body BMC values (g) in WT and *Ctrl*^{+/-} mice throughout the reproductive period. The BMC was significantly reduced in both genotypes at late lactation, but recovered back to baseline after weaning. No significant difference was noted between WT and *Ctrl*^{+/-} mice at any time point.

3.5 Serum and urine minerals assays

To investigate *in vivo* minerals changes that are closely related to BMC changes, I conducted several mineral assays including serum and urine calcium, serum and urine phosphorus and serum and urine magnesium.

3.5.1 Serum total calcium

Serum total calcium concentrations of both WT and *Ctr^{+/-}* mice throughout the reproductive period are shown in Figure 10. Normally, mice serum calcium level does not significantly change during the reproductive period. WT and *Ctr^{+/-}* maintained serum total calcium concentration within the range of 2.1 to 2.4. There was no significant difference between WT and *Ctr^{+/-}* mice at any time point.

3.5.2 Urine calcium

Urine calcium concentrations normalized to urine creatinine are shown in Figure 11. Calcium excretion usually increases during pregnancy due to absorptive hypercalciuria, and decreases during lactation by the effect of PTHrP, which increases calcium renal reabsorption. In this experiment, urine calcium did not increase during pregnancy, but it did decline significantly during lactation to 0.3 ± 0.1 in WT and 0.4 ± 0.1 in *Ctr^{+/-}* ($p < 0.05$ compared with Baseline). *Ctr^{+/-}* mice tended to excrete less calcium in urine than WT at late pregnancy (1.1 ± 0.2 of WT vs. 0.7 ± 0.3 of *Ctr^{+/-}*, $p =$ not significant). By the end of lactation and during post-weaning recovery, urine calcium was similar to Baseline

in both genotypes. No significant differences of urine calcium were observed between WT and *Ctrl*^{+/-} at any time point.

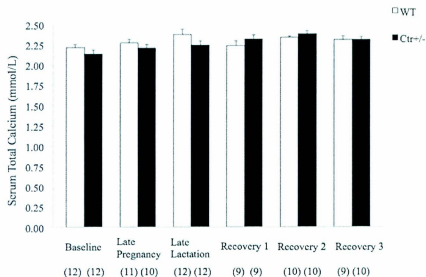


Figure 10: Serum total calcium in WT and *Ctrl^{-/-}* mice throughout reproductive period. Serum total calcium remained relatively stable at every time point during the reproductive period in both groups. WT and *Ctrl^{-/-}* mice shared the same pattern of serum total calcium without any significant difference between them.

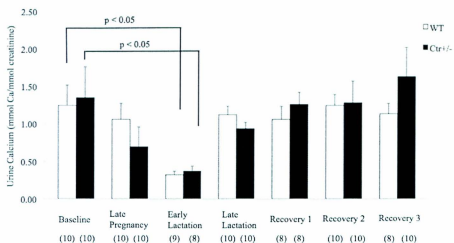


Figure 11: Urine calcium in WT and *Ctrl*^{+/-} mice during reproductive period. Both genotypes had significantly reduced urine calcium excretion during early lactation. No significant differences were observed between WT and *Ctrl*^{+/-} mice at any time point throughout the reproductive period.

3.5.3 Serum phosphorus

Serum phosphorus concentrations of WT and *Ctrl*^{-/-} mice are shown in Figure 12. Phosphorus was unchanged at late pregnancy, but was significantly decreased in both genotypes at late lactation. WT phosphorus concentration declined from 2.5 ± 0.1 to 2.1 ± 0.1 , while *Ctrl*^{-/-} phosphorus fell from 2.5 ± 0.1 to 2.0 ± 0.1 ($p < 0.05$). During post-weaning recovery, the serum phosphorus was normal in both genotypes, although in *Ctrl*^{-/-} mice the serum phosphorus was significantly lower at recovery 1 than at recovery 2 (2.4 ± 0.1 vs. 2.8 ± 0.2 , $p < 0.05$). There were no significant differences between WT and *Ctrl*^{-/-} mice during the reproductive period.

3.5.4 Urine phosphorus

Urine phosphorus values are shown in Figure 13. WT and *Ctrl*^{-/-} mice had the same trend in urine phosphorus changes during the period except at late pregnancy. WT urine phosphorus was unchanged in late pregnancy while *Ctrl*^{-/-} mice showed a significantly decreased urine phosphorus concentration (11.0 ± 2.2 of WT vs. 4.4 ± 1.4 of *Ctrl*^{-/-}, $p < 0.05$). As expected, urine phosphorus by late lactation was significantly increased in WT and *Ctrl*^{-/-}, reaching peak values of 30.1 ± 3.5 and 26.6 ± 6.5 , respectively. After lactation, urine phosphorus returned to the Baseline level in both groups.

3.5.5 Serum magnesium

Serum magnesium concentrations are shown in Figure 14. One small but significant difference was measured. Changes for serum magnesium increased in *Ctrl*^{-/-} mice from

1.2 ± 0.0 at baseline to 1.4 ± 0.1 at late pregnancy ($p < 0.05$). There were no other significant differences within or between genotypes at any time point.

3.5.6 Urine magnesium measurement

Urine magnesium values are shown in Figure 15. WT mice showed significantly increased urine magnesium excretion at late pregnancy (7.9 ± 0.9 at Baseline vs. 12.9 ± 1.0 , $p < 0.05$), but no increase occurred in *Ctrl*^{-/-} mice. Both genotypes had significantly elevated urine magnesium by late lactation, which returned to baseline values by recovery 1. The urine magnesium significantly increased again at recovery 2 and 3. No significant differences were observed between WT and *Ctrl*^{-/-} from baseline to recovery 3.

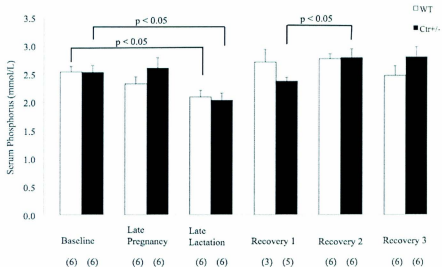


Figure 12: Serum phosphorus in WT and *Ctr*^{+/+} mice throughout the reproductive period. Both had reduced serum phosphorus concentrations at late lactation when compared with baseline ($p < 0.05$). Serum phosphorus in *Ctr*^{+/+} mice seemed to lag behind WT in returning to the baseline level during post-weaning recovery. There were no significant differences between WT and *Ctr*^{+/+} mice at any time point.

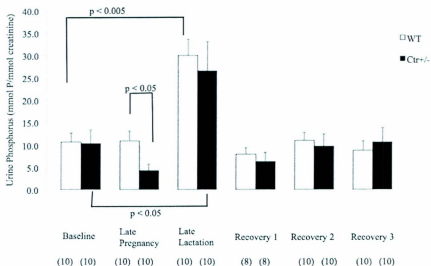


Figure 13: Urine phosphorus in WT and *Ctrl^{-/-}* mice throughout the reproductive period. Urine phosphorus in *Ctrl^{-/-}* was significantly lower than that found in WT at late pregnancy. Both WT and *Ctrl^{-/-}* experienced high urine phosphorus excretion at late lactation ($p < 0.05$), and then the urine phosphorus levels went down to baseline levels during recovery after lactation.

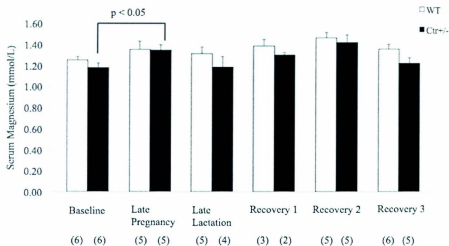


Figure 14: Serum magnesium in WT and *Ctr^{-/-}* mice throughout reproductive period. *Ctr^{-/-}* mice had slightly higher serum magnesium in late pregnancy when compared with baseline ($p < 0.05$). There were no significant differences in serum magnesium concentration between WT and *Ctr^{-/-}* mice at any time point.

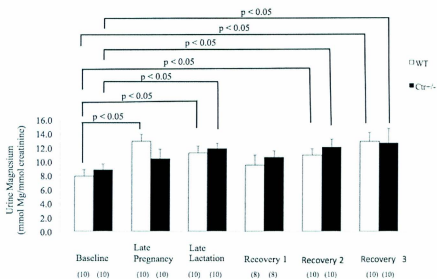


Figure 15: Urine magnesium in WT and *Ctrl*^{+/-} throughout the reproductive period. WT mice increased urine magnesium excretion during pregnancy ($p < 0.05$) whereas no significant increase occurred in *Ctrl*^{+/-} mice. Both groups had higher urine magnesium concentrations at late lactation versus baseline ($p < 0.05$) and at recovery 2 and recovery 3 versus baseline. There were no significant differences between WT and *Ctrl*^{+/-} at any time point.

3.6 Markers of bone turnover assays

Bone turnover markers reflect the relative activity of bone formation and resorption. A serum bone formation marker (P1NP) and a urine bone resorption marker (DPD) were measured.

3.6.1 Serum P1NP assay

Serum P1NP concentrations of WT and *Ptr^{+/+}* mice throughout the reproductive period were shown in Figure 16. P1NP remained at Baseline level during pregnancy and early lactation in both genotypes before increasing significantly at late lactation (197.6 ± 46.1 in WT vs. 193.3 ± 22.3 in *Ptr^{+/+}*) and recovery 1 (136.9 ± 29.6 in WT vs. 375.3 ± 176.5 in *Ptr^{+/+}*) when compared with baseline (66.4 ± 12.5 in WT vs. 51.9 ± 11.4 in *Ptr^{+/+}*). WT and *Ptr^{+/+}* showed the same pattern of serum P1NP changes during the reproductive period without any significant differences between them.

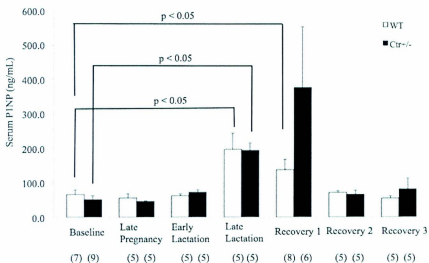


Figure 16: Serum P1NP in WT and *Ctrl*^{-/-} mice throughout the reproductive period. WT and *Ctrl*^{-/-} mice showed normal P1NP during pregnancy and early lactation, but high serum P1NP at late lactation ($p < 0.05$). P1NP remained at a significantly high level in WT mice during recovery 1 ($p < 0.05$). Although the large error bar made the high P1NP at recovery 1 in *Ctrl*^{-/-} mice non-significant, it was still considered a high level. After recovery 1, P1NP returned to the baseline level in both genotypes. No significant differences in serum P1NP between WT and *Ctrl*^{-/-} were observed.

3.6.2 Urine DPD

Urine DPD concentrations are shown in Figure 17. Bone resorption increases during lactation, and this was confirmed by increased urine DPD excretion in WT and *Ctr*^{-/-} mice at early lactation, which became statistically significant at late lactation. Urine DPD increased even further in WT and *Ctr*^{-/-} mice at recovery 1. WT and *Ctr*^{-/-} mice did not have any significant differences between them at any time point.

3.6.3 Serum PTH

Serum PTH values are shown in Figure 18. PTH usually decreases during pregnancy and lactation. In this study, however, PTH increased significantly in both WT and *Ctr*^{-/-} mice during pregnancy and remained elevated during lactation and post-weaning recovery. Although WT mice seemed to have higher PTH than *Ctr*^{-/-} at Baseline (31.6 ± 11.5 in WT and 10.6 ± 4.7 in *Ctr*^{-/-}), the difference was not statistically significant at that or any other time point.

3.7 Milk calcium content

Since an absence of calcitonin altered milk calcium content and *Ctr* is expressed by lactating mammary tissues, milk calcium was assayed in WT and *Ctr*^{-/-} mice and normalized to milk protein content. The results are shown in Figure 19. No significant difference was detected between the two genotypes.

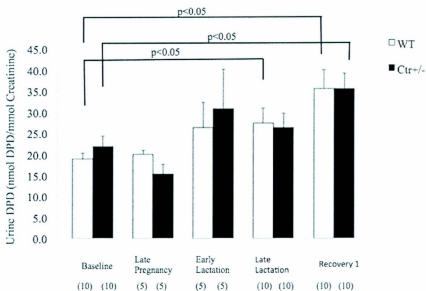


Figure 17: Urine DPD in WT and *Ctr*^{+/-} mice during the reproductive period. In both genotypes, DPD increased during early and late lactation, and increased further during post-weaning recovery. WT and *Ctr*^{+/-} did not show any significant differences at any time point.

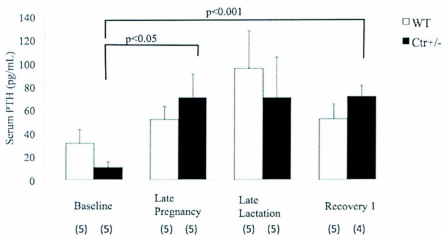


Figure 18: Serum PTH in WT and *Ctr^{+/-}* mice throughout the reproductive period. Although a decrease in PTH was expected during pregnancy and lactation, in both genotypes PTH increased and remained elevated through recovery 1. No significant differences between WT and *Ctr^{+/-}* mice were observed.

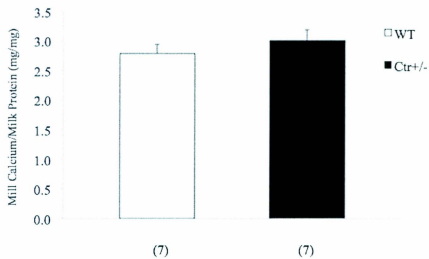


Figure 19: Milk calcium content normalized to milk protein in WT and *Ctr*^{+/-} mice at early lactation. No significant differences between WT and *Ctr*^{+/-} mice were observed.

3.8 Micro computed tomographic (μ CT) analysis of tibias

Considering that there were no significant differences in BMC changes between WT and *Ctr^{+/-}* mice throughout the reproductive period, micro computed tomographic (μ CT) analysis was used to determine whether the two genotypes experienced any different trabecular bone microstructure changes between baseline and late lactation. The results are shown in Table 1. Consistent with increased bone resorption leading to net bone loss, both the WT and *Ctr^{+/-}* group had significantly decreased mean trabecular thickness (MTT), increased trabecular separation, and decreased bone volume/tissue volume (BV/TV) at late lactation ($p < 0.05$). In contrast, bone volume increased by late lactation, and the difference was significant in *Ctr^{+/-}* mice (0.47 ± 0.03 at late lactation vs. 0.36 ± 0.02 at baseline, $p < 0.05$). The two genotypes also had significantly increased bone surface and tissue volume (TV) at late lactation when compared with baseline ($p < 0.05$). No significant differences were detected between WT and *Ctr^{+/-}* mice in any of these parameters.

Table 1: Micro computed tomographic changes in WT and *Ptr^{+/-}* mice at baseline and late lactation (LL)

Veterbrae	MTT (μm)	MTS (μm)	BV (mm^3)	TV (mm^3)	BV/TV (%)	BS (mm^2)
WT baseline (5)	53.31 \pm 1.31 ^a	183.59 \pm 5.25	0.33 \pm 0.02	1.76 \pm 0.11 ^a	19.07 \pm 0.97	26.03 \pm 1.45 ^a
WT LL (5)	48.90 \pm 0.61 ^a	206.46 \pm 17.25	0.43 \pm 0.04	2.80 \pm 0.33 ^a	15.72 \pm 1.64	37.84 \pm 3.02 ^a
<i>Ptr^{+/-}</i> baseline (5)	51.99 \pm 0.73 ^b	194.65 \pm 7.36	0.36 \pm 0.02 ^a	1.99 \pm 0.09 ^b	17.95 \pm 1.12 ^a	28.40 \pm 1.19 ^b
<i>Ptr^{+/-}</i> LL (5)	49.16 \pm 0.22 ^b	207.94 \pm 4.43	0.47 \pm 0.03 ^a	3.17 \pm 0.21 ^b	14.93 \pm 0.48 ^a	41.95 \pm 2.54 ^b

μCT analysis revealed that both genotypes had significantly decreased trabecular bone thickness and increased bone surface at Late Lactation than they had at Baseline stage. *Ptr^{+/-}* mice had increased bone volume but not WT. MTT- mean trabecular thickness, MTS-mean trabecular separation, BV- trabecular bone volume, TV - total volume, BV/TV- trabecular bone volume relative to total volume, BS - trabecular bone surface. Shared letters within *columns* indicate statistical significance ($p < 0.05$). The results were expressed as Mean number \pm SE.

3.9 Biomechanical tests

3.9.1 3-point bend (3PB) test

Tibias from WT and *Ptr^{+/+}* mice at baseline and late lactation were used to test cortical bone strength. Results are shown in Table 2. The ultimate load of force required to break tibias in both WT and *Ptr^{+/+}* was significantly less at late lactation than that at baseline ($p < 0.05$). Consistent with this indication of weaker bone, the tibias of the two genotypes also had reduced stiffness and absorbed less energy prior to breakage. Displacement (distance moved before breakage) also increased in both genotypes, but was significant only in *Ptr^{+/+}* mice. No significant differences were found between WT and *Ptr^{+/+}*.

3.9.2 Reference point indentation test

The reference point indentation test is a relatively new procedure that tests cortical bone strength by reversibly deforming the cortical surface with a microprobe. It has not been tested during lactation, and so this experiment was a trial to determine if the procedure could detect a difference between baseline and end-of-lactation bone strength. Tibias and vertebrae from WT at baseline and late lactation were analyzed; the company declined to analyze bones from *Ptr^{+/+}* mice. Using a standard 2N force, no significant differences in cortical bone strength as indicated by indentation distance increase were detected between baseline and late lactation, with 4.0 ± 0.3 and 5.0 ± 0.5 respectively. However, there was a trend for greater indentation distance, which is the expected result if cortical bone strength is reduced at the end of lactation. Results are shown in Figure 20. The experiment was repeated with a potentially deforming force of 3N and the results were

similar and not statistically significant (not shown). The vertebrae could not be reliably measured due to little resistance to the probe, and so no data were obtained from that analysis.

Table 2: 3-point bend (3PB) test of tibia between WT and *Ptr^{+/+}* at baseline and late lactation (LL)

Genotype and stage	Ultimate load (gf)	Displacement (μm)	Stiffness (gf/mm)	Energy absorbed (gf/mm ²)
WT baseline (4)	2.00 \pm 0.10 ^a	0.45 \pm 0.08	9.77 \pm 0.45 ^a	0.64 \pm 0.03 ^a
WT LL (7)	1.37 \pm 0.12 ^a	0.67 \pm 0.13	7.44 \pm 0.61 ^a	0.44 \pm 0.04 ^a
<i>Ptr^{+/+}</i> baseline (5)	1.80 \pm 0.10 ^b	0.34 \pm 0.05 ^a	9.58 \pm 0.52 ^b	0.57 \pm 0.03 ^b
<i>Ptr^{+/+}</i> LL (8)	1.33 \pm 0.10 ^b	0.78 \pm 0.11 ^a	7.73 \pm 0.44 ^b	0.42 \pm 0.03 ^b

3PB test showed that both WT and *Ptr^{+/+}* mice had weaker bone strength at late lactation than at baseline. Both genotypes had the same trend of bone strength change from baseline to lactation, without any significant difference between them. Shared letters within columns indicate statistical significance ($p < 0.05$). The results were expressed as Mean \pm SE.

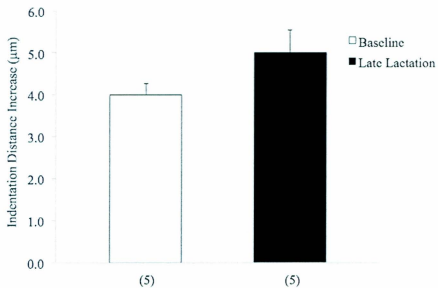


Figure 20: Indentation distance increase of tibias at baseline and late lactation in WT mice. No significant differences in bone strength were found between baseline and late lactation in WT mice.

3.10 *Ctr* mRNA expression analysis

RNA was extracted from bone to determine if CTR mRNA expression is reduced in *Ctr*^{+/-} mice, as was previously shown in other osteoclasts derived from *Ctr*^{+/-} mice studied *in vitro*. Real-time quantitative RT-PCR results were analyzed using the $2^{-\Delta\Delta Ct}$ method (see Figure 21). CTR Ct normalized to GAPDH Ct was used as the indicator of CTR mRNA expression, and the results were normalized to the WT values. No significant fold change was observed between WT and *Ctr*^{+/-} mice, indicating no difference in CTR mRNA expression.

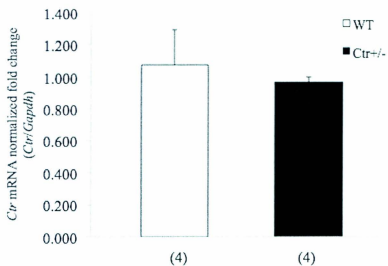


Figure 21: Tibial expression of CTR mRNA in WT and *Ctrl*^{+/-} at baseline. Real-time quantitative RT-PCR showed no significant difference in *Ctrl* mRNA expression between WT and *Ctrl*^{+/-} mice. Tests were conducted in triplicate and normalized to *Gapdh* and the WT value.

4 Discussion

Calcitonin plays an important role in normal calcium and bone metabolism during lactation, since *Ct/cgrp* null mice lacking calcitonin experience more BMC loss during lactation than WT mice (77). Thus calcitonin is physiologically important because it prevents excessive bone resorption during lactation. Whether the same is true in humans is unknown. In this project, I investigated *Ctr^{+/-}* mice to determine whether partial loss of the *Ctr* gene causes the same phenotypes as a loss of calcitonin.

4.1 Phenotypes in mice during the reproductive period

Since bone contains a large amount of mineral, changes in BMC reflect changes in the amount of bone due to formation or resorption. Bone contains 99% of the body's calcium, over 85% of its phosphorus, and 66% of its magnesium. Calcium and phosphorus form hydroxyapatite crystals in bone (84, 120). Together with alterations in circulating levels of bone formation and resorption markers, serum and urine levels of these three minerals can be used as indirect indicators of bone metabolism (99).

The BMC scanning experiments were conducted beginning 10 wk after the mice were born, thus ensuring that the experimental mice had reached peak bone mass (121). WT and *Ctr^{+/-}* mice showed a relatively stable BMC after reaching peak bone mass. At baseline, there was no significant difference between the two with BMC of 0.501 g in WT and 0.520 g in *Ctr^{+/-}*. MicroCT also showed no significant difference in bone phenotypes between the genotypes at baseline. These findings by DXA and microCT differ from the

only prior published report, in which *Ctr^{+/-}* mice were found by microCT to have a higher bone mass than WT. Since, in my studies, sister WT and *Ctr^{+/-}* mice were compared, it could be concluded that there was no difference between the WT and *Ctr^{+/-}* mice. Other parameters were also not different between WT and *Ctr^{+/-}*, including urine and serum minerals, and bone formation and resorption markers. A previous study in our group showed that Blackswiss calcitonin null mice also had the same BMC as WT mice (77). These results may indicate that calcitonin and CTR play unimportant roles in establishing peak bone mass, since absence of the ligand does not alter bone mass in virgin females by 10 wk of age (77).

During pregnancy in mammals, the mother provides calcium for fetal development (99). In order to maintain maternal serum calcium homeostasis, bone may be resorbed to release calcium. However, in my experiments, I observed that a relative change in bone metabolism during pregnancy was an increase in BMC. This may be an adaptation of mammals to store calcium in preparation for the demand of calcium for milk production. The rate of intestinal calcium absorption increases during pregnancy. This helps provide calcium to the fetus and also makes calcium available for the maternal skeleton to increase BMC (105). Both WT and *Ctr^{+/-}* mice had an increase in BMC of the whole body, with a 7.4% increase in WT and 7.7% increase in *Ctr^{+/-}*. In contrast, the lumbar spine lost BMC during pregnancy in both WT and *Ctr^{+/-}* mice while the hind limb gained BMC. The whole body measurement largely reflects changes in cortical bone, while lumbar spine and hind limb contain a mix of trabecular and cortical bone. The lumbar spine contains the largest proportion of trabecular bone. Trabecular bone has much more surface area

than cortical bone, enabling osteoclasts to resorb this form of bone more rapidly than cortical bone. Why the spine resorbs during pregnancy while the whole body and hind limb are gaining BMC is unclear. We have previously found that genetic differences are likely a factor, since Blackswiss mice gain BMC at the whole body level and spine during pregnancy, while C57BL/6 mice (the same strain that *Ctr^{+/-}* mice are in) gain BMC at the whole body level and lose it at the spine during pregnancy (77). The gain in BMC at the hind limb may be a response to increased body weight (increased loading response) during pregnancy that must be borne by the limbs.

During lactation, calcium is required for milk production (99). WT and *Ctr^{+/-}* mice lost BMC of the whole body to maintain maternal serum calcium homeostasis, with a 10.7% decrease in WT and 10.6% decrease in *Ctr^{+/-}* mice, respectively. A further decline in BMC occurred at the lumbar spine during lactation, and the hind limb also lost BMC. Bone resorption releases minerals into serum, and, during lactation, these minerals will either go into milk, be excreted into the urine, or return to the skeleton in the form of newly mineralized bone (99). Urine calcium excretion decreased in both genotypes throughout early lactation and remained low during late lactation, indicating that calcium was not being lost in the urine but instead was being used to produce milk. In contrast, urine phosphorus and magnesium excretion were significantly increased during late lactation. Although hydroxyapatite contains twice as much calcium as phosphorus, it is evident that much of the phosphorus released from bone is not needed for milk production. The excess phosphorus and magnesium released from bone during lactation are excreted into the urine. The bone formation marker PINP and bone resorption marker DPD

increased significantly during lactation in both WT and *Ctrl^{-/-}* mice, confirming that bone turnover was increased. In fact, both increased bone formation and resorption occur during lactation, with resorption exceeding formation, to lead to a net loss of bone as shown by the changes seen in BMC by DXA and by microCT. DPD increases the most during the first ten days of lactation, but this time point was not measured in these experiments; thus the highest level of DPD was not seen nor was the imbalance between resorption and formation markers at this time point. I focused on the end of lactation time point to detect the maximal change in BMC that results, and not the mid-point of lactation when bone resorption occurs at the maximal rate.

The microCT results showed that vertebrae, which are largely composed of trabecular bone, had a significantly increased bone surface area along with a decreased thickness, which is consistent with more osteoclasts resorbing bone when compared to the baseline. Despite the net loss of bone mass, the total volume and bone volume increased by late lactation, whereas the BV/TV decreased as expected (77). This increase in total volume has been observed before in lactating rodents and may be a form of compensation for the loss of bone strength during lactation (77, 122, 123). It implies that periosteal bone formation occurred during pregnancy and lactation to increase the total volume of bone while endosteal resorption occurred during lactation. Consequently, even though less bone is present, the increased bone volume offsets the decline in bone strength somewhat, since a wider cylinder is inherently stronger than a narrower cylinder of the same mass. But, despite this increase in bone volume, bone strength at late lactation was still reduced,

as indicated by the 3PB test. Conceivably, bone strength would have been reduced even further had the compensatory increase in bone volume not occurred.

Ptr^{+/-} mice displayed a significant increase of total volume and bone volume at Late Lactation, while, in WT mice, the increase in total volume was significant, and the increase in bone volume just escaped statistical significance. In both genotypes, the decline in BV/TV was statistically significant. Although there was no direct evidence showing that *Ptr^{+/-}* lost more bone than WT, it is reasonable to speculate that bone microstructure in *Ptr^{+/-}* was weakened more than in WT during lactation, necessitating a greater compensatory increase in bone volume. However, since there were no other differences in bone mass, strength, or volume between WT and *Ptr^{+/-}* mice at any other time point, it is possible that this is a chance finding and not a true difference. Given the trend in bone volume of WT mice to increase by a similar magnitude as in *Ptr^{+/-}* mice, it seems most likely that WT and *Ptr^{+/-}* mice experienced the same changes in bone mass during pregnancy and lactation.

Besides the 3PB test, we also investigated the use of the novel reference point indentation test to analyze cortical bone strength change from baseline to late lactation as a trial analysis to validate the technique. However, we found this technique was not as good as the 3PB test for cortical bone strength analysis because it could not distinguish a difference in bone strength of tibia between baseline and late lactation in WT mice, whereas the 3PB test could. Reference point indentation could not be used on vertebrae at all because the bone was not strong enough even at baseline to yield a consistent result.

BMC in both WT and *Ctrl*^{+/+} mice recovered back to baseline after the bone loss experienced during lactation. A previous study in our group showed that BMC in calcitonin null mice, which lost twice as much BMC as in WT, were able to recover to the non-pregnant level, although the recovery process took just several more days than in WT mice (77). My experimental results show that only one allele of the calcitonin receptor gene is required for post-weaning bone recovery to be achieved. BMC values reached by the end of the post-weaning period were actually increased when compared with the non-pregnant BMC value (shown by Figure 6 – Figure 8). One explanation of this is that the mice had increased BMC with age. Based on previous studies, the recovery period of mice is 3 weeks (21 days) (77). BMC quickly recovered to Baseline level after weaning, and this process usually did not take 3 weeks. Once it reached the baseline level within 3 weeks, BMC kept increasing. BMC data was obtained at the end of each week during recovery. The highest BMC result was used to indicate the level to which bone had recovered, shown in Figure 6 – Figure 8. Although the mean values of absolute BMC values were increased post-weaning over baseline, for both genotypes the difference was non-significant.

Urine and serum minerals remained at the non-pregnant level during post-weaning recovery, except that renal magnesium excretion increased during Recovery 2 and 3 stages. This may be a chance finding, or it may indicate that more magnesium is being absorbed during post-weaning than is required to mineralize the new bone that is being formed. Bone formation and resorption markers were highly increased in both genotypes

during early post-weaning recovery, confirming that bone turnover stays at a higher rate compared to the non-pregnant period. Although bone formation and resorption markers are both increased during early post-weaning recovery, the net effect is the opposite from lactation, with the rate of bone formation exceeding that of bone resorption.

4.2 Roles of *Ctr* in renal phosphorus excretion at late pregnancy

The only significant difference between WT and *Ctr*^{+/-} mice was in a significantly decreased urine phosphorus excretion in *Ctr*^{+/-} mice at late pregnancy, and this was accompanied by a trend for reduced excretion of calcium and magnesium, as well. These results may indicate that loss of one copy of the *Ctr* gene may be sufficient to impair urine phosphorus excretion at late pregnancy, during a time when the net intestinal absorption of phosphorus is likely increased. *Ctr* is expressed in renal tubules, where it is known to play a role in renal mineral excretion. The evidence regarding the function of calcitonin in renal phosphorus handling is quite controversial. One study by Dr. Insogna's group showed that calcitonin administration in X-linked hypophosphatemia increased serum phosphorus and suppressed circulating FGF23, which could increase phosphorus excretion (124). However, another study suggested that calcitonin could inhibit phosphorus reabsorption (125). One example given was that a renal tubular cell line from an American opossum stably transfected with the calcitonin receptor had inhibited intracellular phosphorus reabsorption (more phosphorus loss in urine). But this inhibition is in a tubular cell line specific manner (126). Although I found that haploinsufficiency of *Ctr* did not alter *Ctr* mRNA expression in bone, the same may not be true of kidneys.

Future work will look at *Ctr* gene expression in the kidney to see whether haploinsufficiency of *Ctr* would significantly change the expression level. The lack of one copy of the *Ctr* might lead *Ctr*^{+/-} mice to have impaired renal mineral excretion during late pregnancy, a time when intestinal mineral absorption is increased such that the renal filtered load of these minerals is also increased.

PTH and FGF23 each increase renal phosphorus excretion. During late pregnancy, there was no significant difference in serum PTH between WT and *Ctr*^{+/-}, and so it seems unlikely that altered PTH explains the difference in renal phosphorus excretion in WT and *Ctr*^{+/-} mice. Future work should examine FGF23 and its soluble co-receptor Klotho at late pregnancy between WT and *Ctr*^{+/-} to determine whether haploinsufficiency of *Ctr* leads to altered FGF23 physiology, which could, in turn, alter renal phosphorus excretion. First, serum FGF23 concentration and FGF23 expression at bone tissue in *Ctr*^{+/-} mice will be examined; second, mechanisms of how CTR and FGF23 interact with each other will be studied.

4.3 Parathyroid hormone during reproductive period

PTH and PTHrP both activate the RANKL-RANK pathway to induce osteoclast-mediated bone resorption (44, 46, 47). They have a similar N-terminal structure, enabling both to act on the PTHR. In non-pregnant adults, low serum calcium stimulates synthesis and release of PTH to increase calcium release from bone. In lactating humans, PTH remains at non-pregnant levels or decreases, while PTHrP production is highly increased in

mammary tissue and causes an increase in the circulating PTHrP concentration, as well (107). High PTHrP combines with low estradiol to enhance bone resorption and thereby provide sufficient calcium for milk production. PTHrP measurements are not easily obtained in mice, and so, in this project, I only measured serum PTH.

PTH was measured at baseline, late pregnancy, late lactation, and recovery 1. No significant differences were detected between WT and *Ptr^{+/-}* mice. Within the WT group, there was no significant difference at any time point, while *Ptr^{+/-}* mice had significantly increased PTH at late pregnancy and recovery 1. An increasing trend in PTH levels from baseline to late lactation was observed in both genotypes. Sample size in this experiment was relatively low, with only 5 samples in each experimental group. These findings contrast with the decline in PTH that we have previously observed during pregnancy and lactation in WT mice, and it is unclear why these new data differ from what has previously been obtained in our group (118). Genetic differences are possible, although we have observed a decline in PTH in both Blackswiss and C57 strains in prior experiments. Certainly, the loss of calcium in milk and a low dietary calcium intake can stimulate PTH to increase during lactation, thereby resorbing bone to maintain maternal serum calcium within the normal range. However, the mice in these experiments were maintained on the same diet and conditions that prior mice received in our laboratory, and so the lack of suppression of PTH remains unexplained.

Several reasons may explain the difference in serum PTH change pattern from baseline to late lactation between WT and *Ptr^{+/-}* mice. First, the loss of one copy of *Ptr* might

enhance renal calcium excretion, and a loss of calcium in the urine should lead to a lower serum calcium. In turn, a trend for lower serum calcium will trigger PTH release to restore the serum calcium to normal through PTH's effects on renal tubular calcium handling, bone resorption, and stimulation of calcitriol production. However, urine calcium analysis throughout the reproductive period indicated that *Ctr*^{+/-} mice did not have significantly higher urine calcium than WT mice at any time point. Therefore, this possibility was reasonably excluded, conceding the limitations that random urine samples have when compared to the more thorough collection of all urine when mice are maintained in metabolic cages. Second, *Ctr*^{+/-} might have reduced intestinal calcium absorption, which caused PTH release to stabilize the serum calcium. This explanation was supported by an experiment in 1986 showing that calcitonin elevated calcitriol production, thus increasing intestinal calcium absorption (127). Loss of one copy of *Ctr* may impair calcitriol formation and intestinal calcium absorption, which, in turn, would stimulate a compensatory increase in PTH production throughout reproductive cycle.

4.4 Comparison between *Ctr*^{+/-} and Calcitonin (*Ct/cgrp*) knockout mice throughout the reproductive period

The objective of this research project was to determine whether loss of *Ctr* causes the same phenotype as loss of the ligand calcitonin. However, *Ctr* null mice do not usually survive gestation, and so *Ctr*^{+/-} mice had to be used to compare with WT mice. Studies by Dr. Galson's group (the group that generated these mice) using real-time quantitative PCR, showed that haploinsufficiency of *Ctr* caused a two-fold reduction in *Ctr* expression

in osteoclasts cultured *in vitro* (19). This result was encouraging that $Ctr^{+/-}$ mice would have a phenotype due to reduced *Ctr* mRNA expression. But, after finding no difference in the phenotype between WT and $Ctr^{+/-}$ mice in my experiments, I then analyzed *Ctr* mRNA expression *in vivo*, extracted from tibias, and found that WT and $Ctr^{+/-}$ mice had the same *Ctr* mRNA expression level. Since I measured the *Ctr* expression in the harvested bone tissue directly, this result is more relevant than *Ctr* expression in cultured osteoclasts. Another potential reason why my *Ctr* expression result is different from the one of Dr. Galson's group is that only female mice were used in my research work. Although, in the published paper, it does not mention that both genders were utilized in the study, the possibility that phenotypic differences between male and female mice affect *Ctr* expression cannot be excluded (19). *Ctr* is expressed not only at osteoclasts in bone but also at mammary gland tissue and the pituitary gland. In the mammary gland, the calcitonin/calcitonin receptor signaling pathway appears to suppress PTHrP expression. PTHrP can induce bone resorption during lactation. In the pituitary gland, the pathway may reduce prolactin. Prolactin causes estrogen deficiency and stimulation of PTHrP expression. Therefore, analysis of *Ctr* gene expression at pituitary and mammary gland tissue is necessary as well in the future.

Previous studies showed that calcitonin null mice lost significantly more BMC than WT mice during lactation at the whole body, lumbar spine and tibia regions (77). This was supported by urine DPD analysis, which showed that the null mice had significantly higher DPD than WT mice at late lactation, but these phenotypes were not observed in $Ctr^{+/-}$ mice. Bone microarchitecture analysis by μ CT also did not find any difference

between WT and $Ctr^{+/-}$ mice at any time point. The same result was observed in bone strength, with no difference between WT and $Ctr^{+/-}$ mice. The reason for the lack of a difference in phenotype between WT and $Ctr^{+/-}$ mice is likely because loss of one copy of the gene did not affect *Ctr* gene expression *in vivo*. BMC of both $Ctr^{+/-}$ and calcitonin null mice could recover to baseline level after lactation. This result confirmed, to some extent, that calcitonin signaling through CTR was not required for post-weaning recovery.

It is also possible that serum calcitonin itself could upregulate in response to haploinsufficiency of CTR. However, I did not examine such a possibility at this point because the time needed to collect more serum was not available. However, serum calcitonin level will be measured throughout these main time points of the reproductive cycle. If serum calcitonin is higher in $Ctr^{+/-}$ than in WT mice, it will be evidence of compensation for the loss of one allele of *Ctr* gene.

4.5 Future work

4.5.1 Exploration of *Ctr* knockout mice on Blackswiss strain

We have previously found that the Blackswiss strain, in which the CT mice were studied, rescues the phenotype of some knockout mice, which would otherwise die *in utero*, including the PTH/PTHrP receptor null mice. It is possible that the phenotype of $Ctr^{+/-}$ mice may differ in the Blackswiss background when compared to C57, given that Blackswiss mice begin with a higher bone mass and lose much more bone mass during lactation than C57 mice do. Since few *Ctr* null mice survive to birth in the C57 mice

strain and the reason for this early mortality is unknown, the CTR colony is being backcrossed into the BlackSwiss background to determine if *Ctr* null mice will survive to adulthood. If *Ctr* null mice do not survive, *Ctr*^{+/-} mice in the Blackswiss background will still be studied to determine if loss of one copy of the gene alters the phenotype during pregnancy and lactation as compared to WT mice.

4.5.2 Knockdown experiments

If crossing *Ctr* mice into Blackswiss does not result in any *Ctr* null mice surviving, and if *Ctr*^{+/-} mice in that genotype continue to have no distinctive phenotype, alternative approaches may be developed. Options include trying to knock down the expression of *Ctr* in *Ctr*^{+/-} mice during lactation by using antibodies or siRNAs; however, the length of time required for knockdown in the whole animal during lactation seems prohibitive and unlikely to succeed. Instead, another option would be to create a conditional knockout of *Ctr* that is not induced until after birth. This should really be a global knockout of the *Ctr* after birth in order to ensure that the *Ctr* is knocked out in all tissues, and so an inducible Cre, such as with the Tet-On/Tet-Off system, could be used. Cre is a DNA recombinase that specifically recognizes the loxP sequences in a genome. In the presence of Cre, DNA recombination occurs between the loxP sites, deleting genes between the loxP sites. After Cre is transfected into the genome, if loxP sequences are inserted at either end of a critical exon of *Ctr* using knock-in techniques, the expression of Cre can silence *Ctr* expression. The Tet-On/Tet-Off system can be used to control the expression of Cre. Chemicals such as tetracycline or doxycycline regulate the Tet-On/Tet-Off system. By using the form of

Tet that is always off unless the drug is present, normal *Ctr* expression will be maintained during fetal development through adolescence. Then, doxycycline can be administered to promote Cre expression and eliminate the expression of *Ctr* in the adult mouse prior to mating. In this way, the combination of Cre and the Tet-On/Tet-Off system may enable a global knockout of the *Ctr* after birth. An osteoclast-specific knockout of *Ctr* would not be as useful at first because the phenotype of *Ct/Cgrp* null mice may be the result of loss of calcitonin action in multiple tissues (pituitary, mammary, bone) and not just in bone.

4.5.3 Alternative global *Ctr* knockout that already exists

One research group in Australia created a global inducible *Ctr* knockout that shows normal postnatal survival (128). Those investigators used the Cre system under the control of Cytomegalovirus (CMV) promoter. The CMV promoter was coupled with the Tet-On/Tet-Off system, which regulated the activity of the CMV promoter (129). Insertion of loxP sequences at Exon 13, Exon 14 and the 3' untranslated region (3' UTR) of *Ctr* enabled Cre-mediated suppression of the gene. During fetal development, the CMV promoter was inhibited, leading to no Cre expression. Thus *Ctr* had normal expression, and the fetus survived. After birth, the activity of the CMV promoter was enhanced by regulating the Tet-On/Tet-Off system, thus making Cre largely expressed. The expression of Cre inactivated normal *Ctr* expression by recombining the region between loxP sequences. This enabled the global knockout of *Ctr* in mice. Real-time PCR showed that *Ctr* expression was reduced by over 94%, but not 100%. This animal model

is the best option for studying CTR function during pregnancy and lactation. The only problem is that the investigators have been reluctant to share this model with anyone else.

4.6 Conclusion

WT and *Ctr*^{+/-} underwent similar changes in bone mass, bone microarchitecture, calcitropic hormones, and serum and urine minerals during pregnancy and lactation. After lactation, the skeleton of each genotype recovered fully and quickly.

The loss of one copy of the calcitonin receptor gene did not cause the same phenotype that complete loss of the ligand caused in mice. It may simply be that the loss of one copy is not sufficient to impair calcitonin's role in regulating bone metabolism, especially given that *Ctr* mRNA expression was normal in the tibias of *Ctr*^{+/-} mice. Further work will be needed to study (and generate, if necessary) a model that results in global loss of *Ctr* in animals that survive post natally.

Reference

1. Ott SM 1996 Theoretical and Methodological Approach, In: Bilezikian JP, Raisz LG, and Rodan GA(ed) Principles of Bone Biology, Academic Press, San Diego, CA; pp 231-240
2. Marks SC and Hermey DC 1996 The Structure and Development of Bone, In: Bilezikian JP, Raisz LG, and Rodan GA(ed) Principles of Bone Biology, Academic Press, San Diego, CA; pp 1-13
3. Krause C, deGorter D, Karperien M, and tenDijke P 2008 Signal Transduction Cascades Controlling Osteoblast Differentiation, In: Rosen CJ, Compston JE, and Lian JB(ed) Primer on the Metabolic Bone Diseases and Disorders of Mineral Metabolism, 7 ed. American Society for Bone and Mineral Research, Washington, DC; pp 10-14
4. Ross FP 2008 Osteoclast Biology and Bone Resorption, In: Rosen CJ, Compston JE, and Lian JB(ed) Primer on the Metabolic Bone Diseases and Disorders of Mineral Metabolism, 7 ed. American Society for Bone and Mineral Research, Washington, DC; pp 16-21
5. Bonewald LF 2008 Osteocytes, In: Rosen CJ, Compston JE, and Lian JB(ed) Primer on the Metabolic Bone Diseases and Disorders of Mineral Metabolism, 7 ed. American Society for Bone and Mineral Research, Wahsington, DC; pp 22-26
6. Eriksen EF 2010 Cellular Mechanisms of Bone Remodeling. Rev Endocr Metab Disord 11:219-227.
7. Stein GS and Lian JB 1993 Molecular mechanisms mediating proliferation/differentiation interrelationships during progressive development of the osteoblast phenotype. Endocrine Reviews 14:424-442.
8. Otto F, Thornell AP, Crompton T, Denzel A, Gilmour KC, Rosewell IR, Stamp GWH, Beddington RSP, Mundlos S, Olsen BR, Selby PB, and Owen MJ 1997 Cbfa1, a Candidate Gene for Cleidocranial Dysplasia Syndrome, Is Essential for Osteoblast Differentiation and Bone Development. Cell 89:765-771.
9. Nishio Y, Dong Y, Paris M, O'Keefe RJ, Schwarz EM, and Drissi H 2006 Runx2-mediated Regulation of the Zinc Finger Osterix/Sp7 Gene. Gene 372:62-70.

10. Nakashima K, Zhou X, Kunkel G, Zhang Z, Deng JM, Behringer RR, and deCrombrughe B 2002 The Novel Zinc Finger-Containing Transcription Factor Osterix Is Required for Osteoblast Differentiation and Bone Formation. *Cell* 108:17-29.
11. Spinella-Jaegle S, Roman-Roman S, Dunn CF-W, Kawai S, Galléa S, Stiot V, Blanchet AM, Courtois B, Baron R, and Rawadia G 2001 Opposite Effects of Bone Morphogenetic Protein-2 and Transforming Growth Factor- β 1 on Osteoblast Differentiation. *Bone* 29:323-330.
12. Lee K-S, Kim H-J, Li Q-L, Chi X-Z, Ueta C, Komori T, Wozney JM, Kim E-G, Choi J-Y, Ryoo H-M, and Bae S-C 2000 Runx2 Is a Common Target of Transforming Growth Factor β 1 and Bone Morphogenetic Protein 2, and Cooperation between Runx2 and Smad5 Induces Osteoblast-Specific Gene Expression in the Pluripotent Mesenchymal Precursor Cell Line C2C12. *Mol Cell Biol.* 20:8783-8792.
13. Ross FP and Teitelbaum SL 2005 α v β 3 and Macrophage Colony-stimulating Factor: Partners in Osteoclast Biology. *Immunological Reviews* 208:88-105.
14. Pixley F and Stanley E 2004 CSF-1 Regulation of the Wandering Macrophage: Complexity in Action. *Trends in Cell Biology* 14:628-638.
15. Boyle W, Simonet W, and Lacey D 2003 Osteoclast Differentiation and Activation. *Nature* 423:337-342.
16. Zwerina J, Hayer S, Tohidast-Akrad M, Bergmeister H, Redlich K, Feige U, Dunstan C, Kollias G, Steiner G, Smolen J, and Schett G 2004 Single and Combined Inhibition of Tumor Necrosis Factor, Interleukin-1, and RANKL Pathways in Tumor Necrosis Factor-Induced Arthritis: Effects on Synovial Inflammation, Bone Erosion, and Cartilage Destruction. *Arthritis Rheum.* 50:277-290.
17. Clines G and Guise T 2005 Hypercalcaemia of Malignancy and Basic Research on Mechanisms Responsible for Osteolytic and Osteoblastic Metastasis to Bone. *Endocr Relat Cancer* 12:549-583.
18. Goltzman D, Miao D, Panda DK, and Henty GN 2004 Effects of Calcium and of the Vitamin D System on Skeletal and Calcium Homeostasis: Lessons from

Genetic Models. *The Journal of Steroid Biochemistry and Molecular Biology* 89-90:485-489.

19. Dacquin R, Davey RA, Laplace C, Lévassieur R, Morris HA, Goldring ST, Gebre-Medhin S, Galson DL, Zajac JD, and Karsenty G 2004 Amylin Inhibits Bone Resorption While the Calcitonin Receptor Controls Bone Formation in Vivo. *J Cell Biol* 164:509-514.
20. Granholm S, Lundberg P, and Lerner UH 2007 Calcitonin Inhibits Osteoclast Formation in Mouse Haematopoietic Cells Independently of Transcriptional Regulation by Receptor Activator of NF- κ B and c-Fms. *Journal of Endocrinology* 195:415-427.
21. Nijweide PJ, Burger EH, Nulend JK, and Plas AVd 1996 The Osteocyte, In: Bilezikian JP, Raisz LG, and Rodan GA(ed) *Principles of Bone Biology*, Academic Press, San Diego, CA; pp 115-127
22. Aarden E, Burger E, and Nijweide P 1994 Function of Osteocytes in Bone. *J Cell Biochem* 55:287-299.
23. Tatsumi S, Ishii K, Amizuka N, Li M, Kobayashi T, Kohno K, Ito M, Takeshita S, and Ikeda K 2007 Targeted Ablation of Osteocytes Induces Osteoporosis with Defective Mechanotransduction. *Cell Metabolism* 5:464-475.
24. Heino TJ, Hentunen TA, and Väänänen HK 2002 Osteocytes Inhibit Osteoclastic Bone Resorption through Transforming Growth Factor- β : Enhancement by Estrogen. *J Cell Biochem* 85:185-197.
25. Noble B 2005 Microdamage and apoptosis. *Eur J Morphol* 42:91-98.
26. Al-Dujaili SA, Lau E, Al-Dujaili H, Tsang K, Guenther A, and You L 2011 Apoptotic Osteocytes Regulate Osteoclast Precursor Recruitment and Differentiation in vivo. *J Cell Biochem* 112:2412-2423.
27. Favus M and Goltzman D 2008 Regulation of Calcium and Magnesium, In: Rosen CJ, Compston JE, and Lian JB(ed) *Primer on the Metabolic Bone Diseases and Disorders of Mineral Metabolism*, American Society for Bone and Mineral Research, Washington, DC; pp 104-107

28. Brown E 2008 Ca²⁺-Sensing Receptor In:Rosen CJ, Compston JE, and Lian JB(ed) Primer on the Metabolic Bone Diseases and Disorders of Mineral Metabolism,American Society for Bone and Mineral Research, Wahsington, DC; pp 134-139
29. Fudge NJ and Kovacs CS 2004 Physiological Studies in Heterozygous Calcium Sensing Receptor (CaSR) Gene-ablated Mice Confirm That the CaSR Regulates Calcitonin Release in vivo. BMC Physiol 4:5.
30. Ward D, Brown E, and Harris H 1998 Disulfide Bonds in the Extracellular Calcium-Polyvalent Cation-sensing Receptor Correlate with Dimer Formation and Its Response to Divalent Cations in Vitro. J Biol Chem 274:27642-27650.
31. Hofer A and Brown E 2003 Extracellular Calcium Sensing and Signalling. Nat Rev Mol Cell Biol 4:530-538.
32. Bikle D, Adams J, and Christakos S 2008 Vitamin D: Production, Metabolism, Mechanism of Action, and Clinical Requirements,In:Rosen CJ, Compston JE, and Lian JB(ed) Primer on the Metabolic Bone Diseases and Disorders of Mineral Metabolism,American Society for Bone and Mineral Research, Washington, DC; pp 141-147
33. Amling M, Priemel M, Holzmann T, Chapin K, Rueger JM, Baron R, and Demay MB 1999 Rescue of the Skeletal Phenotype of Vitamin D Receptor-ablated Mice in the Setting of Normal Mineral Ion Homeostasis Formal Histomorphometric and Biomechanical Analyses. Endocrinology 140:4982-4987.
34. Dardenne O, Prud'homme J, Hacking SA, Glorieux FH, and St-Arnaud R 2003 Correction of the Abnormal Mineral Ion Homeostasis with a High-calcium, High-phosphorus, High-lactose Diet Rescues the PDDR Phenotype of Mice deficient for the 25-hydroxyvitamin D-1alpha-hydroxylase (CYP27B1). Bone 32:332-340.
35. Prince C and Butler W 1987 1,25-dihydroxy VitaminD3 Regulates the Biosynthesis of Osteopontin, a Bone-derived Cell Attachment Protein, in Clonal Osteoblast-like Osteosarcoma Cells. Coll Relat Res 7:305-313.
36. Price P and Baukol S 1980 1,25-dihydroxy Vitamin D3 Increases synthesis of the Vitamin K-dependent Bone Protein by Osteosarcoma Cells. J Biol Chem 255:11660-11663.

37. Yasuda H, Shima N, Nakagawa N, Yamaguchi K, Kinosaki M, Mochizuki S, Tomoyasu A, Yano K, Goto M, Murakami A, Tsuda T, Morinaga T, Higashio K, Udagawa N, Takahashi N, and Suda T 1998 Osteoclast Differentiation Factor Is a Ligand for Osteoprotegerin/Osteoclastogenesis-inhibitory Factor and Is Identical to TRANCE/RANKL. *Proc Natl Acad Sci U S A* 95:3597-3602.
38. Drissi H, Pouliot A, Koolloos C, Stein J, Lian J, Stein G, and vanWijnen A 2002 1,25-(OH)₂-vitamin D₃ Suppresses the Bone-related Runx2/Cbfa1 Gene Promoter. *Exp Cell Res* 274:323-333.
39. Bell NH, Stern PH, Pantzer E, Sinha TK, and Deluca HF 1979 Evidence that Increased Circulating 1 α ,25-Dihydroxyvitamin D is the Probable Cause for Abnormal Calcium Metabolism in Sarcoidosis. *J Clin Invest* 64:218-225.
40. Selby PL, Davies M, Marks JS, and Mawer EB 1995 Vitamin D Intoxication Causes Hypercalcaemia by Increased Bone Resorption Which Responds to Pamidronate. *Clin Endocrinol (Oxf)* 43:531-536.
41. Sneddon W, Barry E, Coutermarsh B, Gesek F, Liu F, and Friedman P 1998 Regulation of Renal Parathyroid Hormone Receptor Expression by 1,25-dihydroxyvitamin D₃ and Retinoic Acid. *Cell Physio Biochem* 8:261-277.
42. Raval-Pandya M, Porta A, and Christakos S 1998 Mechanism of Action of 1,25 dihydroxyvitamin D₃ on Intestinal Calcium Absorption and Renal Calcium Transportation, In: Holick M(ed) *Vitamin D Physiology, Molecular Biology and Clinical Applications*, Humana, Totowa, NJ, USA; pp 163-173
43. Omdahl J, Bobrovnikova E, Choe S, Dwivedi P, and May B 2001 Overview of Regulatory Cytochrome P450 Enzymes of the Vitamin D Pathway. *Steroids* 66:381-389.
44. Nissenson R and Juppner H 2008 Parathyroid Hormone, In: Rosen CJ, Compston JE, and Lian JB(ed) *Primer on the Metabolic Bone Diseases and Disorders of Mineral Metabolism*, American Society for Bone and Mineral Research, Washington, DC; pp 123-126
45. Gensure RC, Gardella TJ, and Juppner H 2005 Parathyroid Hormone and Parathyroid Hormone-related Peptide, and Their Receptors. *Biochemical and Biophysical Research Communications* 328:666-678.

46. Kostenuik P and Shalhoub V 2001 Osteoprotegerin A Physiological and Pharmacological Inhibitor of Bone Resorption. *Curr Pharm Des* 7:613-635.
47. Jilka RL, Weinstein RS, Bellido T, Roberson P, Parfitt AM, and Manolagas SC 1999 Increased Bone Formation by Prevention of Osteoblast Apoptosis with Parathyroid Hormone. *J Clin Invest* 104:439-446.
48. Rodriguez M, Felsenfeld AJ, and Llach F 1990 Aluminum Administration in the Rat Separately Affects the Osteoblast and Bone Mineralization. *J Bone Miner Res* 5:59-67.
49. Jilka RL, O'Brien CA, Bartell SM, Weinstein RS, and Manolagas SC 2010 Continuous Elevation of PTH Increases the Number of Osteoblasts via Both Osteoclast Dependent and -Independent Mechanisms. *J Bone Miner Res* 25:2427-2437.
50. Deal C 2004 The Use of Intermittent Human Parathyroid Hormone as a Treatment for Osteoporosis. *Curr Rheumatol Rep* 6:49-58.
51. Silva BC, Costa AG, Cusano NE, Kousteni S, and Bilezikian JP 2011 Catabolic and Anabolic Actions of Parathyroid Hormone on the Skeleton. *J Endocrinol Invest* 34:801-810.
52. Borba VZ and Manas NC 2010 The Use of PTH in the Treatment of Osteoporosis. *Arq Bras Endocrinol Metabol* 54:213-219.
53. deRouffignac C and Quamme G 1994 Renal Magnesium Handling and Its Hormonal Control. *Physiol Rev* 74:305-322.
54. Ba J and Friedman P 2003 Calcium-sensing Receptor Regulation of Renal Mineral Ion Transport. *Cell Calcium* 35:229-237.
55. Hoenderop J, Nilius B, and Bindels R 2005 Calcium Absorption Across Epithelia. *Physiol Rev* 85:373-422.
56. Cochran M, Peacock M, Sachs G, and Nordin BE 1970 Renal Effect of Calcitonin. *Br Med J* 1:135-137.

57. Michigami T 2007 Calcium-sensing Receptor and Hypoparathyroidism. *Clin Calcium* 17:1186-1191.
58. Hoenderop JGJ, Hartog A, Stuiver M, Doucet A, Willems PHGM, and Bindels RJM 2000 Localization of the Epithelial Ca²⁺ Channel in Rabbit Kidney and Intestine. *J Am Soc Nephrol* 11:1171-1178.
59. Peng J-B, Chen X-Z, Berger UV, Vassilev PM, Tsukaguchi H, Brown EM, and Hediger MA 1999 Molecular Cloning and Characterization of a Channel-like Transporter Mediating Intestinal Calcium Absorption. *J Biol Chem* 274:22739-22746.
60. Slepchenko BM and Bronner F 2001 Modeling of Transcellular Ca Transport in Rat Duodenum Points to Coexistence of Two Mechanisms of Apical Entry. *Am J Physiol Cell Physiol* 281:270-281.
61. Benn BS, Ajibade D, Porta A, Dhawan P, Hediger M, Peng J-B, Jiang Y, Oh GT, Jeung E-B, Lieben L, Bouillon R, Carmeliet G, and Christakos S 2008 Active Intestinal Calcium Transport in the Absence of Transient Receptor Potential Vanilloid Type 6 and Calbindin-D9k. *Endocrinology* 149:3196-3205.
62. Haussler MR, Haussler CA, Jurutka PW, Thompson PD, Hsieh J-C, Remus LS, Selznick SH, and Whitfield GK 1997 The Vitamin D Hormone and Its Nuclear Receptor: Molecular Actions and Disease States. *J Endocrinol* 154 Suppl:S57-S73.
63. Cromphaut SJV, Dewerchin M, Hoenderop JGJ, Stockmans I, Herck EV, Kato S, Bindels RJM, Collen D, Carmeliet P, Bouillon R, and Carmeliet G 2001 Duodenal Calcium Absorption in Vitamin D Receptor-knockout mice: Functional and Molecular Aspects. *Proc Natl Acad Sci U S A* 98:13324-13329.
64. Wood RJ, Tchack L, and Taparia S 2001 1,25-Dihydroxyvitamin D₃ Increases the Expression of the CaT1 Epithelial Calcium Channel in the Caco-2 Human Intestinal Cell Line. *BMC Physiol* 1:11.
65. Brenza HL, Kimmel-Jehan C, Jehan F, Shinki T, Wakino S, Anazawa H, Suda T, and DeLuca HF 1998 Parathyroid Hormone Activation of the 25-hydroxyvitamin D₃-1 α -hydroxylase Gene Promoter. *Proc Natl Acad Sci U S A* 95:1387-1391.

66. Copp DH and Cheney B 1962 Calcitonin-A Hormone From the Parathyroid Which Lowers the Calcium-level of the Blood. *Nature* 193:381-382.
67. Copp DH and Cameron EC 1961 Demonstration of a Hypocalcemic Factor (Calcitonin) in Commercial Parathyroid Extract. *Science* 134:2038.
68. Munson PL and Hirsch PF 1966 Thyrocalcitonin: Newly Recognized Thyroid Hormone Concerned with Metabolism of Bone. *Clin Orthop Relat Res* 49:209-232.
69. Hirsch PF, Voelkel EF, and Munson PL 1964 Thyrocalcitonin: Hypocalcemic Hypophosphatemic Principle of the Thyroid Gland. *Science* 146:412-413.
70. Yamamoto Y, Noguchi T, and Takahashi N 2005 Effect of Calcitonin on Osteoclast. *Clin Calcium* 15:147-151.
71. Chakraborty M, Chatterjee D, Gorelick FS, and Baron R 1994 Cell Cycle-dependent and Kinase-specific Regulation of the Apical Na/H Exchanger and the Na, K-ATPase in the Kidney Cell Line LLC-PK1 by Calcitonin. *Proc Natl Acad Sci U S A* 91:2115-2119.
72. Hirsch PF, Lester GE, and Talmage RV 2001 Calcitonin, an Enigmatic Hormone: Does It Have a Function. *J Musculoskelet Neuronal Interact* 4:299-305.
73. Schneider P, Berger P, Kruse K, and Borner W 1991 Effect of Calcitonin Deficiency on Bone Density and Bone Turnover in Totally Thyroidectomized Patients. *J Endocrinol Invest* 14:935-942.
74. Sugino K, Kure Y, Iwasaki H, and Matsumoto A 1992 Does Total Thyroidectomy Induce Metabolic Bone Disturbance. *Int Surg* 77:178-180.
75. Gonzalez DC, Mautalen CA, Correa PH, eTamer E, and eTamer S 1991 Bone Mass in Totally Thyroidectomized Patients. Role of Calcitonin Deficiency and Exogenous Thyroid Treatment. *Acta Endocrinol* 124:521-525.
76. Bucht E, Telenius-Berg M, Lundell G, and Sjoberg HE 1986 Immunoextracted Calcitonin in Milk and Plasma from Totally Thyroidectomized Women. Evidence

- of Monomeric Calcitonin in Plasma During Pregnancy and Lactation. *Acta Endocrinol* 113:529-535.
77. Woodrow JP, Sharpe CJ, Fudge NJ, Hoff AO, Gagel RF, and Kovacs CS 2006 Calcitonin Plays a Critical Role in Regulating Skeletal Mineral Metabolism during Lactation. *Endocrinology* 147:4010-4021.
 78. Adami S 2008 Calcitonin, In: Rosen CJ, Compston JE, and Lian JB (ed) *Primer on the Metabolic Bone Diseases and Disorders of Mineral Metabolism*, American Society for Bone and Mineral Research, Washington, DC; pp 250-251
 79. Takahashi K, Morimoto R, Hirose T, Satoh F, and Totsune K 2011 Adrenomedullin 2/Intermedin in the Hypothalamo-pituitary-adrenal Axis. *J Mol Neurosci* 43:182-192.
 80. Hoff AO, Catala-Lehnen P, Thomas PM, Priemel M, Rueger JM, Nasonkin I, Bradley A, Hughes MR, Ordonez N, Cote GJ, Amling M, and Gagel RF 2002 Increased bone mass is an unexpected phenotype associated with deletion of the calcitonin gene. *J. Clin. Invest.* 110:1849-1857.
 81. Pondel M 2000 Calcitonin and Calcitonin Receptors: Bone and Beyond. *Int J Exp Pathol* 81:405-422.
 82. Gibbons C, Dackor R, Dunworth W, Fritz-Six K, and Caron KM 2007 Receptor Activity-Modifying Proteins: RAMPing up Adrenomedullin Signaling. *Mol Endocrinol* 4:783-796.
 83. Roh J, Chang CL, Bhalla A, Klein C, and Hsu SY 2004 Intermedin Is a Calcitonin/calcitonin Gene-related Peptide Family Peptide Acting Through the Calcitonin Receptor-like Receptor/receptor Activity-modifying Protein Receptor Complexes. *J Biol Chem* 8:7264-7274.
 84. Drezner MK 1996 Phosphorus Homeostasis and Related Disorders, In: Bilezikian JP, Raisz LG, and Rodan GA (ed) *Principles of Bone Biology*, Academic Press, San Diego, CA; pp 263-274
 85. Debiec H and Lorenc R 1988 Identification of Na⁺, Pi-binding Protein in Kidney and Intestinal Brush-border Membranes. *Biochem J* 255:185-191.

86. Deluca HF 2004 Overview of General Physiologic Features and Functions of Vitamin D. *Am J Clin Nutr* 80:16895-16965.
87. Williams K and Deluca H 2007 Characterization of Intestinal Phosphate Absorption Using a Novel in vivo Method. *Am J Physiol Endocrinol Metab* 292:E1917-E1921.
88. Helps C, Murer H, and McGivan J 1995 Cloning, Sequence Analysis and Expression of the cDNA Encoding a Sodium-Dependent Phosphate Transporter from the Bovine Renal Epithelial Cell Line NBL-1. *Eur J Biochem* 228:927-930.
89. Kempson SA, Lotscher M, Kaissling B, Biber J, Murer H, and Levi M 1995 Parathyroid Hormone Action on Phosphate Transporter mRNA and Protein in Rat Renal Proximal Tubules. *Am J Physiol* 268:F784-F791.
90. White KE and Econs MJ 2008 Fibroblast Growth Factor-23, In: Rosen CJ, Compston JE, and Lian JB (ed) *Primer on the Metabolic Bone Diseases and Disorders of Mineral Metabolism*, American Society for Bone and Mineral Research, Washington, DC; pp 112-116
91. Larsson T, Marsell R, Schipani E, Ohlsson C, Ljunggren Ö, Tenenhouse HS, Jüppner H, and Jonsson KB 2004 Transgenic Mice Expressing Fibroblast Growth Factor 23 under the Control of the $\alpha 1(I)$ Collagen Promoter Exhibit Growth Retardation, Osteomalacia, and Disturbed Phosphate Homeostasis. *Endocrinology* 145:3087-3094.
92. Shimada T, Mizutani S, Muto T, Yoneya T, Hino R, Takeda S, Takeuchi Y, Fujita T, Fukumoto S, and Yamashita T 2001 Cloning and Characterization of FGF23 As a Causative Factor of Tumor-induced Osteomalacia. *Proc Natl Acad Sci U S A* 98:6500-6505.
93. Urakawa I, Yamazaki Y, Shimada T, Iijima K, Hasegawa H, Okawa K, Fujita T, Fukumoto S, and Yamashita T 2006 Klotho Converts Canonical FGF Receptor into a Specific Receptor for FGF23 *Nature* 444:770-774.
94. Schlingmann KP, Weber S, Peters M, Nejsum LN, Vitzthum H, Klingel K, Kratz M, Haddad E, Ristoff E, Dinour D, Syrrou M, Nielsen S, Sassen M, Waldegger S, Seyberth HW, and Konrad M 2002 Hypomagnesemia with Secondary

Hypocalcemia Is Caused by Mutations in TRPM6, A New Member of the TRPM Gene Family. *Nature Genetics* 31:166-170.

95. Schmulen AC, Lerman M, Pak CY, Zerwekh J, Morawski S, Fordtran JS, and Vergne-Marini P 1980 Effect of 1,25-(OH)₂D₃ on Jejunal Absorption of Magnesium in Patients with Chronic Renal Disease. *Am J Physiol* 238:G349-G351.
96. Rude RK, Bethune JE, and Singer FR 1980 Renal Tubular Maximum for Magnesium in Normal, Hyperparathyroid, and Hypoparathyroid Man. *J Clin Endocrinol Metab* 51:1425-1431.
97. Hebert SC 1996 Extracellular Calcium-sensing Receptor: Implications for Calcium and Magnesium Handling in the Kidney. *Kidney Int* 50:2129-2139.
98. Riccardi D, Hall AE, Chattopadhyay N, Xu JZ, Brown EM, and Hebert SC 1996 Localization of the Extracellular Ca²⁺/polyvalent Cation-sensing Protein in Rat Kidney. *Am J Physiol* 274:F611-F622.
99. Kovacs CS and Kronenberg HM 2008 Pregnancy and Lactation, In: Rosen CJ, Compston JE, and Lian JB (ed) *Primer on the Metabolic Bone Diseases and Disorders of Mineral Metabolism*, American Society for Bone and Mineral Research, Washington, DC; pp 90-94
100. Heaney RP and Skillman TG 1971 Calcium Metabolism in Normal Human Pregnancy. *J Clin Endocrinol Metab* 33:661-670.
101. Mangin M, Webb AC, Dreyer BE, Posillico JT, Ikeda K, Weir EC, Stewart AF, Bander NH, Milstone L, and Barton DE 1988 Identification of a cDNA Encoding a Parathyroid Hormone-like Peptide From a Human Tumor Associated with Humoral Hypercalcemia of Malignancy. *Proc Natl Acad Sci U S A* 85:597-601.
102. Stewler GJ, Stern PH, Jacobs JW, Eveloff J, Klein RF, Leung SC, Rosenblatt M, and Nissenson RA 1987 Parathyroid Hormone Like Protein from Human Renal Carcinoma Cells. Structural and Functional Homology with Parathyroid Hormone. *J Clin Invest* 80:1803-1807.

103. Philbrick WM, Wysolmerski JJ, Galbraith S, Holt E, Orloff JJ, Yang KH, Vasavada RC, Weir EC, Broadus AE, and Stewart AF 1996 Defining the Roles of Parathyroid Hormone-related Protein in Normal Physiology. *Physiol Rev* 76:127-173.
104. Fudge NJ, Woodrow JP, and Kovacs CS 2006 Pregnancy Rescues Low Bone Mass and Normalizes Intestinal Calcium Absorption in Vdr Null Mice. *J Bone Miner Res* 21(Suppl):S52.
105. Fudge NJ and Kovacs CS 2010 Pregnancy Up-regulates Intestinal Calcium Absorption and Skeletal Mineralization Independently of the Vitamin D Receptor. *Endocrinology* 151:886-895.
106. Liu XS, Ardeshirpour L, VanHouten JN, Shane E, and Wysolmerski JJ 2012 Site-specific Changes in Bone Microarchitecture, Mineralization, and Stiffness during Lactation and after Weaning in Mice. *Journal of Bone and Mineral Research* 27:865-875.
107. Kovacs CS and Kronenberg HM 1997 Maternal-Fetal Calcium and Bone Metabolism During Pregnancy, Puerperium and Lactation. *Endocr Rev* 18:832-872.
108. vanHouten J, Dann P, Stewart A, Watson C, Pollak M, Karaplis A, and Wysolmerski J 2003 Mammary-specific Deletion of Parathyroid Hormone-related Protein Preserves Bone Mass during Lactation. *J Clin Invest* 112:1429-1436.
109. Watney PJM and Rudd BT 1974 Calcium Metabolism in Pregnancy and in the Newborn. *J Obstet Gynaecol Br Commonw* 81:210-219.
110. Law F, Ferrari S, Rizzoli R, and Bonjour JP 1993 Parathyroid Hormone-related Protein and Calcium Phosphate Metabolism. *Pediatr Nephrol* 7:827-833.
111. Arthur SK and Green R 1983 Renal Function During Lactation in the Rat. *J Physiol* 334:379-393.
112. Kent GN, Price RI, Gutteridge DH, Allen JR, Rosman KJ, Smith M, Bhagat CI, Wilson SG, and Retallack RW 1993 Effect of Pregnancy and Lactation on Maternal Bone Mass and Calcium Metabolism. *Osteoporos Int* 3 (Suppl 1):44-47.

113. Gertner JM, Coustan DR, Kliger AS, Mallette LE, Ravin N, and Broadus AE 1986 Pregnancy as State of Physiologic Absorptive Hypercalciuria. *Am J Med* 81:451-456.
114. Seely EW, Brown EM, Demaggio DM, Weldon DK, and Graves SW 1997 A Prospective Study of Calcitropic Hormones in Pregnancy and Post Partum: Reciprocal Changes in Serum Intact Parathyroid Hormone and 1,25-dihydroxyvitamin D. *Am J Obstet Gynecol* 176:214-217.
115. Lund B and Selnes A 1979 Plasma 1,25-dihydroxyvitamin D levels in pregnancy and lactation. *Acta Endocrinol* 92:330-335.
116. Boass A, Garner SC, Schultz VL, and Toverud SU 1997 Regulation of Serum Calcitriol by Serum Ionized Calcium in Rats During Pregnancy and Lactation. *J Bone Miner Res* 12:909-914.
117. Polatti F, Capuzzo E, Viazzo F, Colleoni R, and Klersy C 1999 Bone Mineral Changes during and after Lactation. *Obstet Gynecol* 94:52-56.
118. Kirby B, Ardeshirpour L, Woodrow J, Wysolmerski J, Sims N, Karaplis A, and Kovacs C 2011 Skeletal Recovery after Weaning Does Not Require PTHrP. *J Bone Miner Res* 26:1242-1251.
119. Laplace C, Li X, Goldring SR, and Galson DL 2002 Homozygous Deletion of the Murine Calcitonin Receptor Gene Is an Embryonic Lethal 24th Annual Meeting of the American Society for Bone and Mineral Research, San Antonio, Texas, USA Presentation No.1175
120. Rude RK 1996 Magnesium Homeostasis, In: Bilezikian JP, Raisz LG, and Rodan GA(ed) *Principles of Bone Biology*, Academic Press, San Diego, CA; pp 277-289
121. Guan M, Yao W, Liu R, Lam KS, Nolte J, Jia J, Panganiban B, Meng L, Zhou P, Shahnazari M, Ritchie RO, and Lane NE 2012 Directing Mesenchymal Stem Cells to Bone to Augment Bone Formation and Increase Bone Mass. *Nature Medicine* 18:456-462.

122. Miller SC, Shupe JG, Redd EH, Miller MA, and Omura TH 1986 Changes in Bone Mineral and Bone Formation Rates during Pregnancy and Lactation in Rats. *Bone* 7:283-287.
123. Vajda EG, Bowman BM, and Miller SC 2001 Cancellous and Cortical Bone Mechanical Properties and Tissue Dynamics during Pregnancy, Lactation, and Postlactation in the Rat. *Biol Reprod* 65:689-695.
124. Liu ES, Carpenter TO, Gundberg CM, Simpson CA, and Insogna KL 2011 Calcitonin Administration in X-linked hypophosphatemia. *N Engl J Med* 364:1678-1680.
125. Carney SL 1997 Calcitonin and Human Renal Calcium and Electrolyte Transport. *Miner Electrolyte Metab* 23:43-47.
126. Muff R, Kaufmann M, Born W, and Fischer JA 1994 Calcitonin Inhibits Phosphate Uptake in Opossum Kidney Cells Stably Transfected with a Porcine Calcitonin Receptor. *Endocrinology* 134:1593-1596.
127. Jaeger P, Jones W, Clemens TL, and Hayslett JP 1986 Evidence That Calcitonin Stimulates 1,25-dihydroxyvitamin D Production and Intestinal Absorption of Calcium in vivo. *J Clin Invest* 78:456-461.
128. Davey RA, Turner AG, McManus JF, Chiu WM, Tjahjono F, Moore AJ, Atkins GJ, Anderson PH, Ma C, Glatt V, MacLean HE, Vincent C, Bouxsein M, Morris HA, Findlay DM, and Zajac JD 2008 Calcitonin Receptor Plays a Physiological Role to Protect Against Hypercalcemia in Mice. *J Bone Miner Res* 23:1182-1193.
129. Baron U, Freundlieb S, Gossen M, and Bujard H 1995 Co-regulation of Two Gene Activities by Tetracycline via a Bidirectional Promoter. *Nucleic Acids Research* 23:3605-3606.

